Check for updates

Advanced MR Techniques for Preoperative Glioma Characterization: Part 1

Lydiane Hirschler, PhD,[1] Nico Sollmann, MD, PhD,[2,3,4] Bárbara Schmitz-Abecassis, MSc,[5,6] Joana Pinto, PhD,[7] Fatemehsadat Arzanforoosh, MSc,[8] Frederik Barkhof, MD, PhD,[9,10] Thomas Booth, MD, PhD,[11,12] Marta Calvo-Imirizaldu, MD,[13] Guilherme Cassia, MD,[14] Marek Chmelik, PhD,[15] Patricia Clement, PhD,[16,17] Ece Ercan, PhD,[5] Maria A. Fernández-Seara, PhD,[13,18] Julia Furtner, MD, PhD,[19,20] Elies Fuster-Garcia, PhD,[21] Matthew Grech-Sollars, PhD,[22,23] Nazmiye Tugay Guven, MSc,[24] Gokce Hale Hatay, MSc,[24] Golestan Karami, PhD,[11] Vera C. Keil, PhD,[9,25] Mina Kim, PhD,[26] Johan A. F. Koekkoek, MD, PhD,[27,28] Simran Kukran, MSc,[29,30] Laura Mancini, PhD,[23,31] Ruben Emanuel Nechifor, PhD,[32] Alpay Özcan, PhD,[33] Esin Ozturk-Isik, PhD,[24]

View this article online at wileyonlinelibrary.com. DOI: 10.1002/jmri.28662

Received Dec 22, 2022, Accepted for publication Feb 9, 2023.

*Address reprint requests to: G.H., Währinger Gürtel 18-20, 1090 Vienna, Austria.
E-mail: gilbert.hangel@meduniwien.ac.at

From the [1]C.J. Gorter MRI Center, Department of Radiology, Leiden University Medical Center, Leiden, The Netherlands; [2]Department of Diagnostic and Interventional Radiology, University Hospital Ulm, Ulm, Germany; [3]Department of Diagnostic and Interventional Neuroradiology, School of Medicine, Klinikum rechts der Isar, Technical University of Munich, Munich, Germany; [4]TUM-Neuroimaging Center, Klinikum rechts der Isar, Technical University of Munich, Munich, Germany; [5]Department of Radiology, Leiden University Medical Center, Leiden, The Netherlands; [6]Medical Delta Foundation, Delft, The Netherlands; [7]Institute of Biomedical Engineering, Department of Engineering Science, University of Oxford, Oxford, UK; [8]Department of Radiology & Nuclear Medicine, Erasmus MC, Rotterdam, The Netherlands; [9]Department of Radiology & Nuclear Medicine, Amsterdam UMC, Vrije Universiteit, Amsterdam, The Netherlands; [10]Queen Square Institute of Neurology and Centre for Medical Image Computing, University College London, London, UK; [11]School of Biomedical Engineering and Imaging Sciences, King's College London, London, UK; [12]Department of Neuroradiology, King's College Hospital NHS Foundation Trust, London, UK; [13]Department of Radiology, Clínica Universidad de Navarra, Pamplona, Spain; [14]Hospital Santa Luzia, Rede D'Or São Luiz, Brasília, Brazil; [15]Department of Technical Disciplines in Medicine, Faculty of Health Care, University of Prešov, Prešov, Slovakia; [16]Department of Diagnostic Sciences, Ghent University, Ghent, Belgium; [17]Department of Medical Imaging, Ghent University Hospital, Ghent, Belgium; [18]IdiSNA, Instituto de Investigación Sanitaria de Navarra, Pamplona, Spain; [19]Department of Biomedical Imaging and Image-guided Therapy, Medical University of Vienna, Vienna, Austria; [20]Research Center of Medical Image Analysis and Artificial Intelligence, Danube Private University, Krems an der Donau, Austria; [21]Biomedical Data Science Laboratory, Instituto Universitario de Tecnologías de la Información y Comunicaciones, Universitat Politècnica de València, Valencia, Spain; [22]Centre for Medical Image Computing, Department of Computer Science, University College London, London, UK; [23]Lysholm Department of Neuroradiology, National Hospital for Neurology and Neurosurgery, University College London Hospitals NHS Foundation Trust, London, UK; [24]Institute of Biomedical Engineering, Bogazici University Istanbul, Istanbul, Turkey; [25]Cancer Center Amsterdam, Amsterdam, The Netherlands; [26]Centre for Medical Image Computing, Department of Medical Physics & Biomedical Engineering and Department of Neuroinflammation, University College London, London, UK; [27]Department of Neurology, Leiden University Medical Center, Leiden, The Netherlands; [28]Department of Neurology, Haaglanden Medical Center, The Hague, The Netherlands; [29]Department of Bioengineering, Imperial College London, London, UK; [30]Department of Radiotherapy and Imaging, Institute of Cancer Research, London, UK; [31]Department of Brain Repair and Rehabilitation, Institute of Neurology, University College London, London, UK; [32]Department of Clinical Psychology and Psychotherapy, International Institute for the Advanced Studies of Psychotherapy and Applied Mental Health, Babes-Bolyai University, Cluj-Napoca, Romania; [33]Electrical and Electronics Engineering Department, Bogazici University Istanbul, Istanbul, Turkey; [34]Department of Mechanical Engineering, Faculty of Natural Sciences and Engineering, Istinye University Istanbul, Istanbul, Turkey; [35]Department of Biophysics, Medical College of Wisconsin, Milwaukee, Wisconsin, USA; [36]Department of Physics and Computational Radiology, Oslo University Hospital, Oslo, Norway; [37]Department of Physics, University of Oslo, Oslo, Norway; [38]Department of Imaging Physics, Delft University of Technology, Delft, The Netherlands; [39]Faculty of Engineering and Design, Atlantic Technological University (ATU) Sligo, Sligo, Ireland; [40]Mathematical Modelling and Intelligent Systems for Health and Environment (MISHE), ATU Sligo, Sligo, Ireland; [41]Department of Radiology, Stanford University, Stanford, California, USA; [42]Stanford Cardiovascular Institute, Stanford University, Stanford, California, USA; [43]Department of Neurosurgery, St. Anne's University Hospital, Brno, Brno, Czech Republic; [44]Faculty of Medicine, Masaryk University, Brno, Czech Republic; [45]Department of Neuroradiology, Hospital Garcia de Orta, Almada, Portugal; [46]Brain Tumour Centre, Erasmus MC Cancer Institute, Rotterdam, The Netherlands; [47]Helmholtz-Zentrum Dresden-Rossendorf, Institute of Radiopharmaceutical Cancer Research, Dresden, Germany; [48]Department of Neurosurgery, Medical University of Vienna, Vienna, Austria; [49]High Field MR Centre, Department of Biomedical Imaging and Image-guided Therapy, Medical University of Vienna, Vienna, Austria; [50]Christian Doppler Laboratory for MR Imaging Biomarkers, Vienna, Austria; and [51]Medical Imaging Cluster, Medical University of Vienna, Vienna, Austria

Additional supporting information may be found in the online version of this article

This is an open access article under the terms of the Creative Commons Attribution License, which permits use, distribution and reproduction in any medium, provided the original work is properly cited.

© 2023 The Authors. *Journal of Magnetic Resonance Imaging* published by Wiley Periodicals LLC on behalf of International Society for Magnetic Resonance in Medicine.

Senol Piskin, PhD,[34] Kathleen Schmainda, PhD,[35] Siri F. Svensson, MSc,[36,37] Chih-Hsien Tseng, PhD,[6,38] Saritha Unnikrishnan, PhD,[39,40] Frans Vos, PhD,[6,8,38] Esther Warnert, PhD,[8] Moss Y. Zhao, PhD,[41,42] Radim Jancalek, PhD,[43,44] Teresa Nunes, MD, PhD,[45] Kyrre E. Emblem, PhD,[36] Marion Smits, MD, PhD,[7,8,46] Jan Petr, PhD,[47] and Gilbert Hangel, PhD[48,49,50,51]*

Preoperative clinical magnetic resonance imaging (MRI) protocols for gliomas, brain tumors with dismal outcomes due to their infiltrative properties, still rely on conventional structural MRI, which does not deliver information on tumor genotype and is limited in the delineation of diffuse gliomas. The GliMR COST action wants to raise awareness about the state of the art of advanced MRI techniques in gliomas and their possible clinical translation or lack thereof. This review describes current methods, limits, and applications of advanced MRI for the preoperative assessment of glioma, summarizing the level of clinical validation of different techniques. In this first part, we discuss dynamic susceptibility contrast and dynamic contrast-enhanced MRI, arterial spin labeling, diffusion-weighted MRI, vessel imaging, and magnetic resonance fingerprinting. The second part of this review addresses magnetic resonance spectroscopy, chemical exchange saturation transfer, susceptibility-weighted imaging, MRI-PET, MR elastography, and MR-based radiomics applications.
Evidence Level: 3
Technical Efficacy: Stage 2

J. MAGN. RESON. IMAGING 2023;57:1655–1675.

Gliomas are a heterogeneous group of neuroepithelial tumors arising from the glial cells, with an age-adjusted average rate of 6.03 per 100,000 population.[1] Traditionally, they are divided according to a four-step grading system where a higher grade represents disease with more malignant features and a mostly dismal prognosis. The traditional concept of the World Health Organization (WHO) grading system based on histopathological assessment underwent significant changes in the fifth edition of the WHO Classification of Tumors of the Central Nervous System (CNS), published in 2021.[2] This current classification introduced revisions to tumor nomenclature and advances the integral role of molecular diagnostics for tumor classification and grading that predicts the prognosis better[3] than the previous 2016 version.[4]

Compared with the 2016 version, the WHO 2021 classification incorporates more molecular alterations into the diagnostics and divides gliomas into adult-type diffuse gliomas, pediatric-type diffuse low-grade (LGG) and high-grade (HGG) gliomas, circumscribed astrocytic gliomas, glioneuronal and neuronal tumors, and ependymal tumors. The primary genetic markers used for glioma taxonomy are now considered isocitrate dehydrogenase (IDH) 1 and 2 mutation status, 1p/19q co-deletion, H3F3A alterations, ATRX gene mutations, O6-Methylguanine-DNA Methyltransferase (MGMT) promoter methylation status, loss of CDKN2A, epidermal growth factor receptor (EGFR) amplification, a combined gain of chromosome 7 and loss of chromosome 10, and TERT promoter pathogenic variants. In adults, the term glioblastoma is now reserved only for IDH-wildtype tumors and will always be graded as 4, whereas IDH-mutated astrocytomas present a distinct progressive disease with WHO grade rising from 2 to 4. As a third class, oligodendrogliomas are now distinct from astrocytomas by possessing both IDH mutation and 1p/19q co-deletion and can range form grade 2 to 4 as well. As the genetic profile of a particular tumor affects its metabolic pathways leading to a certain product or a change in the cell's phenotype, advanced magnetic resonance imaging (MRI) techniques can be a very promising noninvasive approach to predict glioma type and behavior.

Preoperative glioma imaging by MRI is essential to localize and delineate the tumor volume and to assess infiltrative behavior or compressive effects on adjacent structures with related complications. The minimal recommendation for such routine structural imaging protocols at 3T consists of T1-weighted imaging (before and after the administration of gadolinium-based contrast agents (GBCA), 1 mm isotropic resolution), T2-weighted imaging (after GBCA administration, <3 mm slice thickness), T2-weighted fluid-attenuated inversion recovery imaging (<3 mm slice thickness), and diffusion-weighted imaging (<3 mm slice thickness, *b*-values of 0, 500, and 1000 s/mm^2), with further details to be found in Ellingson et al.[5]

With the advent of advanced sequences, quantitative imaging of multiple pathophysiological features in the tumor and surrounding tissue became possible,[6,7] providing the opportunity to noninvasively characterize different molecular types of glioma against the background of the WHO 2021 classification.[6,8] While glioma genotyping based on tissue probes derived from neurosurgical tumor resection or biopsy remains the standard, predicting genotypes by preoperative advanced MRI could aid in clinical decision-making and facilitate individual management tailored to the individual tumor characteristics.[6,9]

In most clinical settings for preoperative glioma assessment, however, only conventional MRI is performed. The untapped potential of advanced MRI seems related to a

15222586, 2023, 6, Downloaded from https://onlinelibrary.wiley.com/doi/10.1002/jmri.28662 by Imperial College London, Wiley Online Library on [24/05/2023]. See the Terms and Conditions (https://onlinelibrary.wiley.com/terms-and-conditions) on Wiley Online Library for rules of use; OA articles are governed by the applicable Creative Commons License

multitude of obstacles that prevent its wider translation into the clinical routine.[10] A major hurdle is the lack of rigorous validation of advanced MRI-derived biomarkers. Although recommendations for the acceleration of imaging biomarker development in cancer, both for lesion segmentation and imaging biomarker quantification, do exist, almost no regulatory qualifications or specific guidelines of high quality have been adopted.[11–13] Finally, advanced sequences beyond conventional structural MRI may require special hardware and/or software combined with the need for dedicated expertise for acquisition, post-processing, and evaluation.[14] This makes advanced imaging of gliomas time-consuming, often involving manual data handling and dedicated, custom-made processing pipelines.

The purpose of this review is to raise awareness and contribute to clinical translations of advanced MRI techniques by describing the methods and application of different modalities for the preoperative assessment of glioma, and summarizing whether these techniques can be routinely used. The first part of this review includes perfusion imaging by dynamic contrast-enhanced (DCE), dynamic susceptibility contrast (DSC), and arterial spin labeling (ASL), as well as diffusion MRI, vessel imaging, and relaxometry and MR fingerprinting (MRF). The second part of this review describes MR spectroscopy, chemical exchange saturation transfer (CEST), susceptibility-weighted imaging (SWI), MRI-PET, MR elastography (MRE), and MR-based radiomics and artificial intelligence (AI) applications. For each technique, we aimed to provide a concise methodological overview, review the strengths and weaknesses of glioma characterization and tumor heterogeneity mapping, and use this as the basis for assessing the level of technical readiness of each method.

Methods

This review was initiated through the European Cooperation in Science and Technology (COST) Glioma MR Imaging 2.0 (GliMR) initiative,[10] which brought together clinicians, engineers, and physicists with expertise in advanced MRI techniques applied to brain tumor imaging in a series of virtual and onsite meetings from July 2020 through September 2022. We defined the target audience of this review as clinicians (eg, neuroradiologists, neurosurgeons, and (neuro-) oncologists) and researchers without deep knowledge of advanced MRI who want to broaden their routine or experimental protocols for brain tumor imaging. We used the GliMR consortium's technical expertise to aggregate the available evidence and level of validation for cutting-edge MRI methods and the information derivable from these.

These advanced MRI techniques allow (semi)quantitative imaging of tumor composition, metabolism, physiology, or mechanical properties that are not captured in routine clinical protocols. At the same time, we included only acquisition, reconstruction, and postprocessing methods that have already demonstrated pilot results in brain tumors.

As this review cannot be a complete review of the literature, all topical experts were instructed to select recent peer-reviewed publications indexed in the MEDLINE database, including reviews that described the techniques with the highest potential impact. Together with a brief technological introduction for every topic, this was intended as a base for our evaluation of the methodological readiness of preoperative advanced MRI methods for future clinical practice.

The methodologies/contrasts within the scope of the work were determined as DCE/DSC, ASL, diffusion MRI, vessel imaging, and MRF—included in the first part of the review—and MRS, CEST, SWI, MR-PET, MRE, and MR-based radiomics—included in the second part. The reviews for these specific sequences were designed to include the following:

- An *Overview* of the technique with links to detailed reviews and recommendations for implementation and use;
- An overview of the current evidence about the *Clinical application* to brain tumor imaging, focusing on how it can be used for glioma characterization and grading according to the new WHO 2021 classification criteria and its focus on molecular characteristics to distinguish between different molecular glioma subtypes, namely oligodendroglioma, IDH-mutant, and 1p/19q co-deleted, astrocytoma, IDH-mutant, and glioblastoma, IDH-wildtype, as well as the improved mapping of structural, functional, and metabolic glioma heterogeneity;
- A statement on the level of clinical and technological *Validation* of the method, summarizing the current status and the prospect for near-future improvements;
- A *Summary* of the recommended use.

The expert panel composed of the authors has addressed the level of validation of all techniques. First, a survey was sent to all the experts, which included questions on the acquisition, processing, and clinical evidence of each method for pre-treatment glioma characterization. If there was a lack of consensus in the answers, the expert panel reviewed the recent literature. After multiple consensus meetings, the level of validation of each technique was summarized in a table (Table 1) that included relevant literature references. Table 2 summarizes specifically the clinical applications of all presented MRI methods for the prediction of molecular glioma subtypes defined in the WHO 2021 classification.

Results

DSC-MRI

OVERVIEW. DSC-MRI entails the acquisition of T2 or T2*-weighted images with a high temporal resolution during which a GBCA is bolus-injected. A gradient-echo echo planar

15222586, 2023, 6, Downloaded from https://onlinelibrary.wiley.com/doi/10.1002/jmri.28662 by Imperial College London, Wiley Online Library on [24/05/2023]. See the Terms and Conditions (https://onlinelibrary.wiley.com/terms-and-conditions) on Wiley Online Library for rules of use; OA articles are governed by the applicable Creative Commons License

TABLE 1. Level of validation table

	Track & Domain[a]	Perfusion			Diffusion				●	■	▲	×
		DSC	DCE	ASL	ADC	DTI	VSI	MRF				
Technical validation												
Test–retest repeatability	T2	●	●	■	■	■	■	■	Yes, with current standard implementation	Yes, but with other implementation or patient group/animal model	None available	Unclear
Cross-vendor reproducibility	T2	●	▲	■	■	■	▲	▲	Yes, with current standard implementation	Yes, but with other implementation or patient group	None available	Unclear
Multi-site reproducibility	T3	●	■	■	■	■	■	■	Yes, with current standard implementation	Yes, but with other implementation or patient group, phantom or analysis	None available	Unclear
Clinical evidence												
Proof-of-concept in patients	C1	●	●	●	●	■	●	■	Differentiation tumor types/grades	Differentiation of tumor from normal brain	None available	Unclear
Evaluated in clinical studies	C2-3	●	●	●	●	●	●	■	Multiple single center	Few or preliminary studies	None available	Unclear
Evaluated in multi-center studies	C3	●	●	■	●	●	●	▲	Good quality with relevant question	Small, preliminary or only method stability/not relevant question	None available	Unclear
Evaluated in meta-analysis		●	●	●	●	■	■	▲	Consistent result with standard measure	Not standard measure/method, or low number of studies/patients	None available	Unclear
Established diagnostic accuracy, cut-offs/criteria	C3	●	●	■	●	■	■	▲	Consistent in multiple single-center studies	Few or preliminary studies	None available	Unclear
Acceptance												
Method guidelines recommendations	T	●	●	●	●	●	■	▲	Available and updated		None available	Unclear

15222586, 2023, 6, Downloaded from https://onlinelibrary.wiley.com/doi/10.1002/jmri.28662 by Imperial College London, Wiley Online Library on [24/05/2023]. See the Terms and Conditions (https://onlinelibrary.wiley.com/terms-and-conditions) on Wiley Online Library for rules of use; OA articles are governed by the applicable Creative Commons License

TABLE 1. Continued

	Track & Domain[a]	Perfusion			Diffusion				●	■	▲	×
		DSC	DCE	ASL	ADC	DTI	VSI	MRF				
										Available, but not updated or not specific for tumor imaging		
Included in national imaging guidelines		●	■	■	●	■	×	×	Endorsed by a majority of the community	Only endorsed by a minority	Not mentioned	Unclear
Included in clinical trial guidelines[b]		●	▲	▲	●	●	■	▲	Included in suggested standard protocol	Mentioned, but clinical value uncertain	Not mentioned	Unclear
Included in international clinical guidelines[c]		■	▲	▲	●	●	■	▲	Endorsed by major international society guidelines	Mentioned, but clinical value uncertain	Not mentioned	Unclear
In clinical use for brain tumor imaging[d]		●	■	▲	●	■	▲	▲	Widely implemented (>50%)	Intermediate (<50%)	Uncommon	Unclear
In clinical use for glioma diagnosis[d]		■	■	▲	●	■	▲	▲	Widely applied (>50%)	Intermediate (<50%)	Uncommon	Unclear
Implementation												
Sequence availability	T2	●	●	●	●	●	●	■	Comparable sequence available as clinical from all major vendors	No standard implementation or only WIP	Research sequence at singles sites	Unclear
Post-processing software availability	T2	●	■	●	●	●	■	●	On-line scanner/reading workstation with best practice implementation	Off-line, commercially available software	In-house software	Unclear
Subjective ease of data acquisition (scanner operator)	T2	■	■	■	●	●	●	●	Minimal need for training	Special training/attention required	Difficult to obtain good quality data	Unclear
Subjective ease of post-processing (within clinical department)		■	■	●	●	■	■	●	No post-processing needed	Extra processing/training needed, but not time consuming	Expert or time intensive processing required	Unclear

15222586, 2023, 6, Downloaded from https://onlinelibrary.wiley.com/doi/10.1002/jmri.28662 by Imperial College London, Wiley Online Library on [24/05/2023]. See the Terms and Conditions (https://onlinelibrary.wiley.com/terms-and-conditions) on Wiley Online Library for rules of use; OA articles are governed by the applicable Creative Commons License

TABLE 1. Continued

Track & Domain[a]	Perfusion			Diffusion						
	DSC	DCE	ASL	ADC	DTI	VSI	MRF	●	■	▲	✕
Subjective ease of data interpretation (clinician)	■	●	■	●	■	■	✕	Visual reading or only simple manual steps required	Special training/expertise required	Highly specialized in single centers	Unclear

(a) Imaging biomarker roadmap; (b) RANO, iRANO, Standardized Brain Tumor Imaging Protocol; (c) GBM EANO/SNO, EANO diff. glioma, EANO glioma; (d) European survey of advanced MRI, US survey of perfusion imaging. T technical validation C clinical validation, Domain 1 Discovery, Domain 2 Validation, Domain 3 Qualification. References to the guidelines and also further material for each technique are included in the supplementary materials.

imaging (GRE-EPI) sequence, heavily T2*-weighted, is most often used. With GBCA confined to the vessels, as for the brain with an intact blood-brain barrier (BBB), a gradient of susceptibility between the intra- and extravascular tissue is induced, causing a transient shortening of the dynamic T2*-weighted signal (S(t)). The S(t) is converted into the relaxation rate change ($\Delta R2 \times (t)$), which, when integrated (added up), provides a voxelwise estimate of the relative cerebral blood volume (rCBV) (relative to the rest of the brain). In addition, voxelwise cerebral blood flow (CBF) can be estimated if the $\Delta R2 \times (t)$ from large arteries (i.e., the arterial input function [AIF]) is also separately measured and used, along with the tissue $\Delta R2 \times (t)$. Since rCBV is the most common DSC-MRI parameter used to evaluate brain tumors (Fig. 1), the remaining discussion will focus on rCBV.

Estimation of rCBV can be confounded by the extravasation of GBCA through a disrupted BBB, a common condition in brain tumors. While this "leakage effect" violates the assumption of GBCA vascular compartmentalization, DSC-MRI can still be successfully used to estimate brain tumor rCBV if this leakage effect is appropriately considered.[15–17] A recent consensus on DSC-MRI data acquisition for brain tumors resulted in two recommended approaches.[18] The first, and most robust approach incorporates a GBCA pre-dose to diminish T1 leakage effects that might occur during the subsequent DSC-MRI acquisition. A second GBCA dose is administered during the collection of the DSC-MRI data, using either a low (30°) or intermediate (60°) flip angle and field strength-dependent TEs (40–50 msec at 1.5T, 25–35 msec at 3T). The second approach has the advantage of not requiring a GBCA pre-dose while using a low flip angle (30°) and field-strength-dependent TEs (1.5T: 40–50 msec; 3T: 25–35 msec). For both approaches, a TR = 1000–1500 msec is recommended, and the inclusion of a post-processing, the contrast-agent leakage correction method is required. While the Boxerman-Schmainda-Weiskoff (BSW) method[16] for leakage correction is most commonly used, other methods have also been proposed.[19–21]

CLINICAL APPLICATION. Studies have shown that rCBV ratios can predict glioma grade[15,22–24] and are able to stratify patients into low, intermediate, and high-risk groups, with shorter survival corresponding to higher rCBV.[25] Both intratumoral and peri-tumoral rCBV were shown to be reliable for the preoperative distinction of HGG from LGG with excellent sensitivity and accuracy.[26] Similarly, delineations of preoperative rCBV "habitats" within both contrast-enhancing and peritumoral regions were found to be highly prognostic for patients who underwent standard-of-care treatment.[27]

Possibly, one of the most significant roles of preoperative rCBV is to assist with ensuring an accurate diagnosis as the heterogeneity of gliomas can lead to misdiagnosis and undergrading. Brain tumor rCBV has been shown helpful in identifying such cases retrospectively,[25] or, preferably,

15222586, 2023, 6, Downloaded from https://onlinelibrary.wiley.com/doi/10.1002/jmri.28662 by Imperial College London, Wiley Online Library on [24/05/2023]. See the Terms and Conditions (https://onlinelibrary.wiley.com/terms-and-conditions) on Wiley Online Library for rules of use; OA articles are governed by the applicable Creative Commons License

TABLE 2. Summary of clinical applications for the prediction of molecular subtypes in gliomas as presented in this review

Methodology	Parameters	Molecular Marker	References
DSC	rCBV	IDH mutation	Lu (2021)
DSC	rCBV	MGMT methylation	Lu (2021)
DCE	K^{trans}, V_e	IDH mutation	Hu (2020)
DCE	K^{trans}	MGMT methylation	Zhang (2017)
ASL	CBF	IDH mutation	Yoo (2020)
ASL	CBF	MGMT methylation	Yoo (2020)
ASL	CBF	p53 expression	Mao (2020)
DWI	ADC	IDH mutation	Leu (2017); Wang (2021)
DWI	ADC	1p/19q co-deletion	Leu (2017)
VAI	CMRO2, MTI	IDH mutation	Stadlbauer (2017)
MRF	T2	IDH mutation	Kern (2020)
MRF	T1	IDH mutation	Springer (2022)

both can be avoided altogether by identifying the best sites for surgical biopsy.[28] In a more recent case report,[29] rCBV class maps (referred to as fractional tumor burden maps), which delineate regions of low, intermediate, and high vascularity (Fig. 2), confirmed that tissue obtained from areas of zero to low rCBV received a histopathologic diagnosis of non-tumor while the remaining unresectable tissue, with a high pre-operative rCBV, was the site of early and aggressive recurrence. Thus, knowledge of the spatial variation in rCBV in both resected and the remaining tissue is fundamental for an accurate diagnosis and follow-up treatment management.

Pre-operative rCBV may also play an important role in the success of the 2016 WHO classification that newly includes molecular markers. Despite the known heterogeneities, at both the cellular and molecular levels, patient stratification and treatment are generally determined on the basis of molecular markers present in a single tumor specimen. As a result, the power of this new classification is being profoundly underutilized and may explain why, even with the advances of molecular profiling, the improvements in patient outcome have been modest.[30] As a potential solution, rCBV was able to predict differences in IDH1 mutation and MGMT status,[31] and tissue from hypercellular and hypervascular microfoci revealed greater expression of Ki-67, HIF-1a, CD31, and EGFR compared to tumor background.[32] Therefore, rCBV has the potential to guide surgical biopsy and provide a more accurate diagnosis for both histopathological and molecular analyses.

VALIDATION. Existing evidence reveals that rCBV is a valuable, and even necessary adjunct to standard MRI. Yet, it has been argued that rCBV remains limited in its clinical adoption due to a lack of standardization, which may explain the variability in reported rCBV thresholds.[33] Still, in recent years several well-curated studies have demonstrated excellent repeatability, cross-site consistency, and market availability, suggesting a high technology readiness level for rCBV.

With DSC-MRI data collected twice within 8 days, in HGG patients, rCBV was found to be highly repeatable.[34] The within-patient coefficient of variation was further reduced when using a standardization algorithm that precluded the need for a user-defined reference region, which is required to normalize rCBV to normal brain values. Similar results were found in a multi-site clinical trial, for which rCBV repeatability was again shown to be excellent with standardized rCBV more repeatable than normalized rCBV.[35]

With multi-site analysis of a shared DSC-MRI dataset, but using several different analysis platforms, rCBV was also able to distinguish high-grade from low-grade glioma in all cases.[36] Moreover, a single threshold, applicable to all platforms, could be identified. This study further suggested that much of the previous variability in reported thresholds may be due to differences in data pre-processing, patient populations, or image acquisition settings, variables that were held fixed in this multi-site study. Moreover, widespread implementation of the recommended acquisition protocol[18] could greatly improve consistency in reported rCBV data, including thresholds by which to distinguish tumor grades. Indeed, two independent sites, using the same acquisition and post-processing methods, were able to arrive at the same threshold to distinguish tumor from treatment effect, validated with spatially matched biopsies.[37,38]

15222586, 2023, 6, Downloaded from https://onlinelibrary.wiley.com/doi/10.1002/jmri.28662 by Imperial College London, Wiley Online Library on [24/05/2023]. See the Terms and Conditions (https://onlinelibrary.wiley.com/terms-and-conditions) on Wiley Online Library for rules of use; OA articles are governed by the applicable Creative Commons License

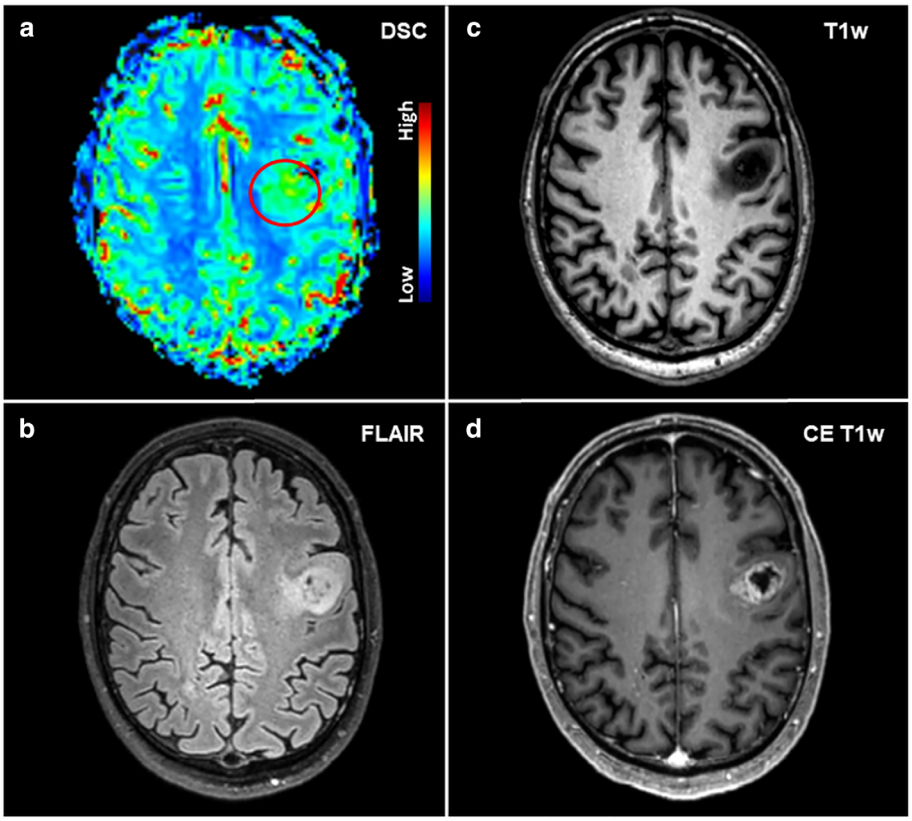


FIGURE 1: Elevated perfusion according to dynamic susceptibility contrast (DSC) MRI (a) in a 55-year-old male patient with a left frontal high-grade glioma (HGG) that showed high signal on fluid-attenuated inversion recovery (FLAIR); (b) imaging and contrast enhancement on T1-weighted imaging (c, axial non-contrast, and d, axial contrast-enhanced images). The borders of the lesion with contrast-enhancing tumor parts, in particular, showed hyperperfusion on DSC MRI (red circle, a).

Finally, FDA-cleared and CE-marked platforms for the analysis of rCBV data are now widely available, with studies published that compared platforms.[36,39,40] Using one such platform, the ease-of-use and ability to collect and analyze multi-site rCBV data were demonstrated by incorporation into clinical trials, with each showing the utility of rCBV to predict outcomes.[35,41,42]

Challenges that remain for DSC-MRI include optimization of the imaging method itself. For example, GRE-EPI can experience signal dropout in regions near air-tissue interfaces, bone, or resection cavities, making it difficult to evaluate tumors in these regions fully. Technical improvements that enable higher spatial resolution imaging and reduced sensitivity, or correction of the unwanted susceptibility effects, are needed. Also, GRE-EPI retains a high sensitivity to large normal vessels, which can make it difficult to evaluate tumor-specific vascularity in these regions. Approaches that combine

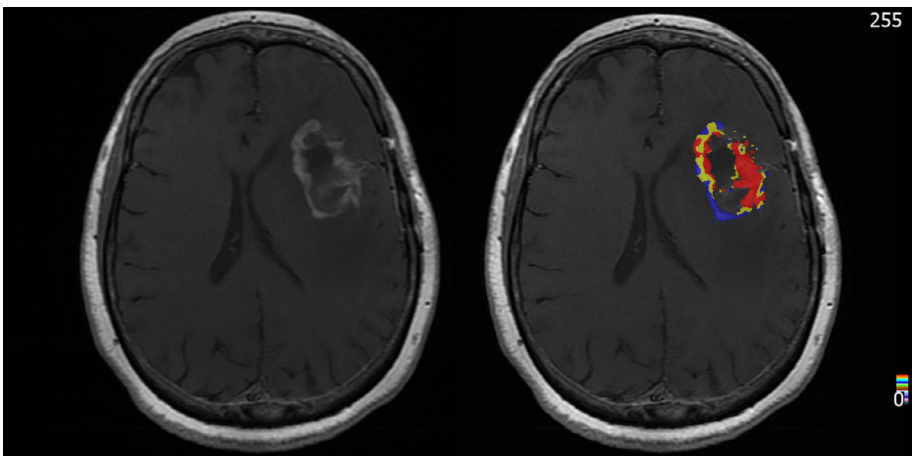


FIGURE 2: Patient with recurrent glioblastoma. (a) T1w MRI with CEA, (b) corresponding map of fractional tumor burden (FTB) showing regions of zero-low (blue), intermediate (yellow), and high rCBV (red)within the contrast agent enhancing region.

15222586, 2023, 6, Downloaded from https://onlinelibrary.wiley.com/doi/10.1002/jmri.28662 by Imperial College London, Wiley Online Library on [24/05/2023]. See the Terms and Conditions (https://onlinelibrary.wiley.com/terms-and-conditions) on Wiley Online Library for rules of use; OA articles are governed by the applicable Creative Commons License

GRE-EPI and SE-EPI[15,17,24,43] may be a solution, as this could offer images with differing vessel size sensitivity and a more complete interpretation. However, such sequences are not yet available for clinical use. Finally, the high temporal resolution required for DSC-MRI often precludes whole-brain imaging. Newer methods that incorporate advances in parallel and simultaneous multi-slice imaging may offer a solution.[44]

SUMMARY. The collection of pre-operative DSC-MRI data with the generation of rCBV maps is easy to obtain and has been shown to be invaluable for the diagnosis and treatment management of glioma. Full clinical adoption should be accelerated with the recent consensus recommendation for DSC-MRI data acquisition and convergence of analysis methods, thus overcoming previous concerns regarding standardization. The remaining issues include improving image quality and coverage.

DCE

OVERVIEW. Dynamic contrast-enhanced MRI (DCE-MRI) is a perfusion technique that monitors the GBCA-induced T1-shortening effect in blood plasma and tissue, if leakage occurs. The signal records mixed information about blood perfusion, vessel permeability, and a fraction of extracellular extravascular space (EES), and is often used to characterize tumor microvasculature. The signal can be assessed semi-quantitatively by evaluating the contrast arrival time, time to the peak, maximum intensity, the area under the curve, wash-in slope, and wash-out rate. Alternatively, a quantitative analysis is achieved by applying tracer kinetic models.[45] The most frequently applied model in tumor assessment is the extended Tofts model, which asserts that the contrast tracer distributes over two compartments: the intravascular space and the EES, with a bi-directional exchange of the tracer across the blood vessel wall.[46] The model enables numerical estimation of the volume transfer constant between the blood plasma and the EES (K^{trans}), the reflux exchange rate from the EES to the blood plasma (K_{ep}), the volume fraction of plasma (V_p), and the volume fraction of EES (V_e) (Fig. 3). The volume transfer constant, K^{trans}, which reflects the vascular permeability, is the most often applied DCE parameter in the context of glioma.[48] General guidelines for applying DCE imaging in pre-clinical research have been summarized in multiple papers.[49,50]

CLINICAL APPLICATION. Malignant gliomas are characterized by a remarkable increase in blood vessel formation (angiogenesis) which leads to aberrant vascular structure, abnormal blood flow, and increased permeability in vessels. DCE-driven parameters were investigated to be potential markers of angiogenic activity in gliomas and are therefore being used for tumor monitoring.[51] An extended systematic review[52] summarized 14 studies about the discrimination between LGGs and HGGs and five studies about the differentiation between primary CNS lymphomas and HGGs based on DCE parameters. The paper concluded that all these studies demonstrated considerable specificity and sensitivity in relation to the studied aspects, showing high diagnostic accuracy in discriminating between LGGs and HGGs (AUC 0.96) and slightly lower performance for discriminating between primary CNS lymphomas and HGGs (AUC 0.86).

Moreover, studies revealed that DCE-driven parameters were able to predict some of the molecular characteristics used recently for the classification of glioma tumors, including IDH and MGMT methylation. Hu et al reported statistically significant differences in histogram parameters of K^{trans} and V_e between IDH-mutated and IDH-wild-type glioma.[53] Furthermore, Zhang et al found that glioblastoma with MGMT methylation showed significantly higher K^{trans}, indicating that MGMT methylation may be involved in glioma-associated angiogenesis characterized by high endothelial permeability vasculatures.[48] The prognostic value of DCE parameters has also been studied, with some studies showing higher K^{trans} and V_e to be associated with worse overall survival (OS), and Ulyte et al showing that high V_e is a consistent predictor of worse progression-free survival and OS in HGG patients.[54]

VALIDATION. DCE MRI has been studied for over three decades. An overwhelming amount of papers have demonstrated the importance of DCE MRI for diagnosis, prognosis, and therapy monitoring in glioma patients. However, one limitation is that the DCE parameters may vary across vendors and systems, hindering cross-center comparison. The variability of DCE parameters results from several factors including different field strengths, imaging principles, sequence settings, and analysis software. Kim has discussed the sources of variability in quantitating DCE parameters and proposed several possible solutions.[55] Hence, a consensus for the implementation of DCE imaging with reduced bias across multi-centers is still needed to facilitate the integration of the DCE technique into standard-of-care imaging in the clinic.

The selection of pharmacokinetic models is also a key factor that influences the DCE parameters. Complex models with fewer assumptions are physiologically more reliable than simpler models, which often make assumptions to constrain the model. Such assumptions may not be appropriate and could bias estimated parameters from the model. Conversely, complex models are more sensitive to noise than simpler models.[56]

SUMMARY. Preclinical and clinical studies have shown that the quantitative DCE MRI parameters could be image biomarkers in glioma imaging. However, it is not yet possible to use DCE MRI as a regular tool in the clinic due to the variability resulting from differences in scanners, sequences, and software. Besides, improving the acquired DCE image quality

15222586, 2023, 6, Downloaded from https://onlinelibrary.wiley.com/doi/10.1002/jmri.28662 by Imperial College London, Wiley Online Library on [24/05/2023]. See the Terms and Conditions (https://onlinelibrary.wiley.com/terms-and-conditions) on Wiley Online Library for rules of use; OA articles are governed by the applicable Creative Commons License

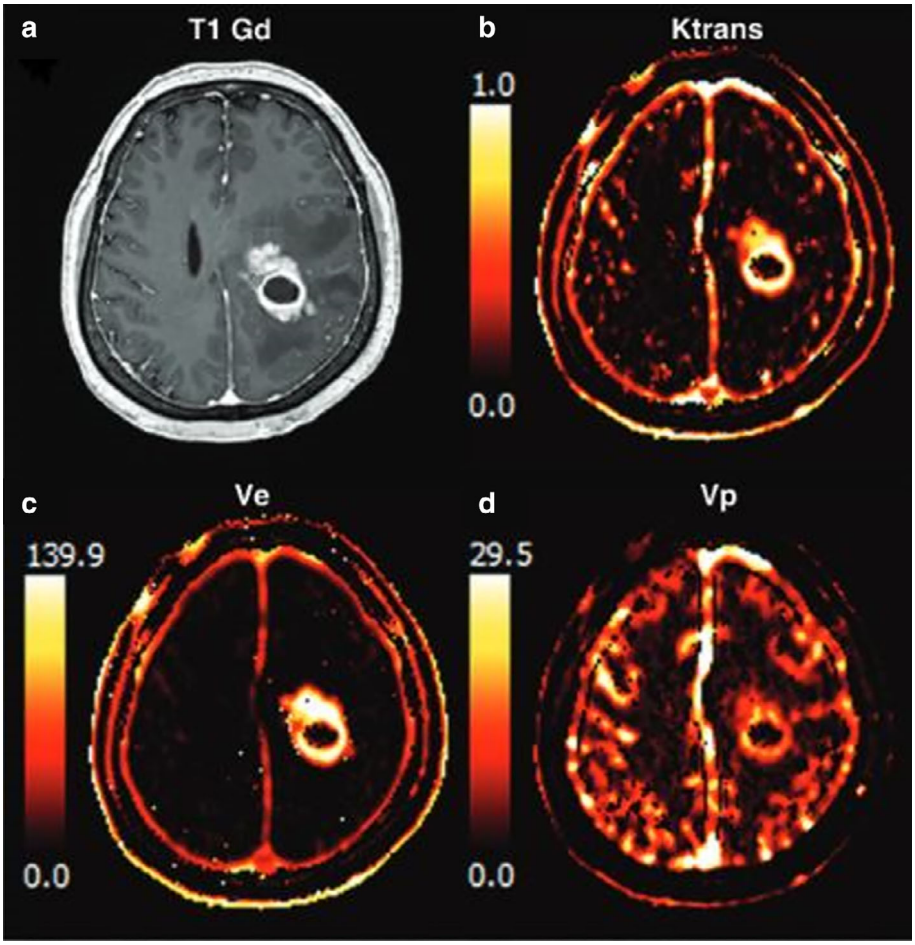


FIGURE 3: The contrast-enhanced T1-weighted image (a) and dynamic contrast-enhanced-derived vascular parameter maps: K^{trans} (b), V_e (c), and V_p (d) of a glioblastoma patient treated with concurrent radiation therapy and temozolomide chemotherapy.[47]

would facilitate the implementation of complex models, which are more realistic in pathological conditions, and further provides more reliable and precise DCE parameters.

ASL

OVERVIEW. ASL magnetically labels arterial blood water by an inversion pulse proximal to the imaging region. After a short delay on the order of seconds, called the post-labeling delay, an image is acquired in the brain, which will be affected by the inflow of inverted spins in blood. The difference between an image acquired with and without this labeling subtracts the tissue signal and only contains the signal from the inflowing blood, allowing quantification of the volume of labeled blood delivered to each voxel.[57] To gain sufficient signal, the measurement has to be repeated several times.

This technique allows absolute quantification of CBF, without the need for the administration of an intravenous contrast media.[57] Given its noninvasive nature, ASL can be easily repeated, implemented in conventional MR protocols, and used in specific populations, such as children, patients with allergic reactions to gadolinium, and patients with kidney failure, where the injection of GBCA would be contraindicated. ASL-MRI has shown good repeatability both within sessions and between sessions with sessions days to months apart.

CLINICAL APPLICATION. Multiple studies have shown the role of ASL in diagnosis, grading, and preoperative planning.[58] In general, ASL detects increased blood flow in glioma[59] and has a high diagnostic value in distinguishing glioma from metastases, primary CNS lymphoma, and non-neoplastic brain lesions.[60]

Two meta-analyses indicated that ASL may be useful in distinguishing HGG and LGG,[61,62] with the maximum tumor blood flow relative to contralateral healthy tissue demonstrating the best discrimination performance.[59] HGG typically exhibits high perfusion and vascularity, consistent with the higher metabolism of the tumor tissue, and shows an above-average signal on ASL. In contrast, LGG tends to demonstrate lower-than-average blood flow (with pilocytic astrocytoma and ganglioglioma the exceptions).[58,60] In addition, ASL has been reported to predict IDH1, MGMT promoter methylation (i.e., higher perfusion), and p53 status

15222586, 2023, 6, Downloaded from https://onlinelibrary.wiley.com/doi/10.1002/jmri.28662 by Imperial College London, Wiley Online Library on [24/05/2023]. See the Terms and Conditions (https://onlinelibrary.wiley.com/terms-and-conditions) on Wiley Online Library for rules of use; OA articles are governed by the applicable Creative Commons License

(i.e., lower perfusion),[63,64] and appears to be correlated with tumor microvascular density[65] and VEGF expression.[66] Nonetheless, more studies related to the specific classification of gliomas with ASL are needed.[59] Finally, ASL can be used for prognosis prediction of patients with glioblastoma, as low-perfused gliomas appear to be associated with longer event-free and OS.[64] Moreover, malignant progression in patients with grade 2 glioma can be predicted using ASL.[67]

VALIDATION. The 2015 ISMRM Perfusion Study Group ASL recommendations resulted from a major effort to standardize ASL for clinical applications in the brain.[57] The suggested 3D pseudo-continuous sequence with background suppression has been adopted by all major scanner vendors and is still considered optimal for ASL in glioma. Labeling duration of 1800 msec, post-labeling delay 2000 msec, basic subtraction calculation, and normalization to contralateral GM values are recommended (Lindner et al MRM 2022, in revision, reference will be added during this manuscript's revision). More research is needed to confirm the added value of multiple post-labeling delays.[68]

Although ASL images suffer from a lower signal-to-noise ratio than the DSC counterpart, a high correlation was found between ASL-derived CBF and DSC-measured rCBV in gliomas,[69] with velocity-selective ASL presenting even better results than normal pseudo-continuous ASL.[70] A comparison is shown in Fig. 4. The lack of expertise in reading ASL images by the radiologist is one of the major hurdles,[14] and more training and tools, together with a more solid validation of ASL, are needed to demonstrate its ability to provide a valid alternative for DSC.

SUMMARY. Absolute measures of tumor blood flow can be obtained with ASL in the absence of exogenous intravenous contrast agents and the sequence is technically ready for clinical use. There is a correlation between ASL-calculated CBF with tumor histology, grade, and microvascular density and no confusion with BBB leakage as in the post-contrast T1-weighted images. However, the added value to the conventional protocol and with respect to DSC still has to be proven in large multi-center studies and diagnostic criteria need to be defined.

Diffusion

OVERVIEW. Diffusion MRI is a technique based on motion-sensitizing magnetic field gradients (*b*-values), which attenuate the signal according to the motion direction and magnitude. Specifically, diffusion models are designed to mathematically estimate the attenuation that originates from the Brownian motion guided by the tissue's microstructure. The quantification of diffusion can then be used as a marker of pathology since the movement of water is dependent on parameters that affect the microstructure, such as cellularity, viscosity, or tortuosity of the extracellular space.

The most frequent method for measuring diffusion is the diffusion-weighted EPI pulse sequence due to its speed and availability, but non-EPI techniques (eg, turbo SE imaging or steady-state free precession) can overcome some of the EPI limitations (eg, geometric warping in areas of susceptibility changes, such as bone/tissue interfaces).

The impedance of water molecule diffusion can be quantitatively assessed using the apparent diffusion coefficient (ADC) by eliminating the T2-weighting that reduces the multi-directional diffusivity at each point into a single number. In current clinical practice, diffusion tensor imaging (DTI) is also commonly used, enabling extraction of quantitative measures, such as fractional anisotropy (FA), or mean diffusivity (MD). FA is a measure of the dispersion of diffusion directionality, which is theoretically 0 in locations where water can freely diffuse in all directions and approaching 1 in highly anisotropic conditions where water diffuses along a single main axis (eg, in densely packed WM fibers). MD is mathematically

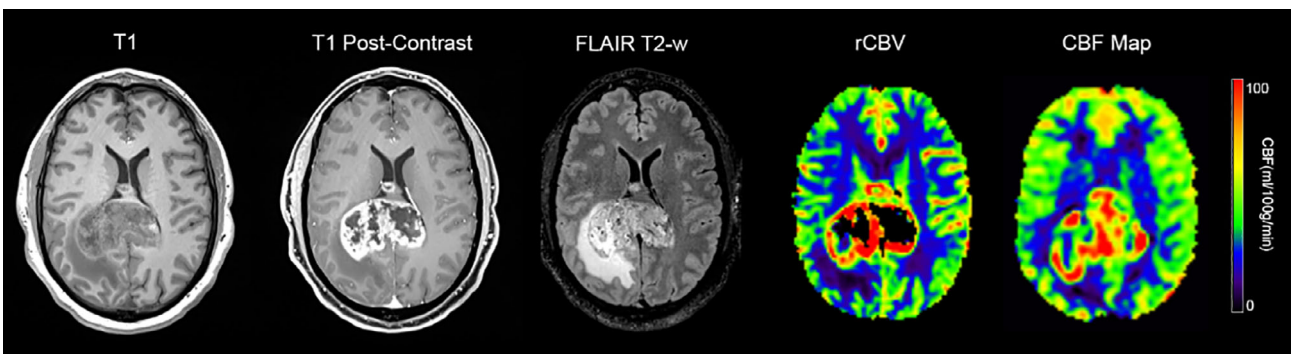


FIGURE 4: MRI results from a 48-year-old patient with a biopsy-proven grade 4 glioblastoma. (Left-to-right) pre-contrast T1-weighted; post-contrast T1-weighted; T2-weighted FLAIR images; relative cerebral blood volume (rCBV) map derived from dynamic susceptibility contrast (DSC) sequence; and cerebral blood flow (CBF) map derived from arterial spin labeling (ASL) are shown for a representative image slice. This example illustrates that the ASL CBF map is comparable to DSC rCBV imaging, showing high perfusion values at the periphery of the lesion. Note the partial volume effect on the central portion of the lesion on the CBF map that underestimates the necrotic area.

15222586, 2023, 6, Downloaded from https://onlinelibrary.wiley.com/doi/10.1002/jmri.28662 by Imperial College London, Wiley Online Library on [24/05/2023]. See the Terms and Conditions (https://onlinelibrary.wiley.com/terms-and-conditions) on Wiley Online Library for rules of use; OA articles are governed by the applicable Creative Commons License

similar to ADC and is a measure of the amount of diffusion in a given volume as an average of diffusion in all directions.

Besides DTI, less common diffusion-MRI techniques include diffusion kurtosis imaging (DKI) and intravoxel incoherent motion (IVIM) imaging. In DKI, the deviation of diffusion from a Gaussian distribution can be quantified by kurtosis, a statistical measure that describes the non-Gaussian behavior in biological tissues. The metrics most commonly extracted are mean kurtosis (MK, average of the diffusion kurtosis along all directions), axial kurtosis (kurtosis along the axial direction), and radial kurtosis (kurtosis along the radial direction). When higher *b*-values are used (eg, $b > 1500$ s/mm^2), kurtosis is more sensitive to microstructural environments and shorter molecular distances. IVIM imaging assumes a pure diffusion component and a pseudo-diffusion component originating from the perfusion, and where multiple *b*-values are used to obtain information on tissue microcirculation (perfusion) and microstructure (diffusion). The main objective of IVIM imaging is to disentangle the effects of perfusion and diffusion in MRI data to generate maps of true diffusion, pseudo-diffusion coefficients, and of microvascular volume fractions.

CLINICAL APPLICATION. Regarding the preoperative quantitative assessment of glioma by diffusion MRI, ADC values could reflect tumor cellularity and the tumor burden (Fig. 5).

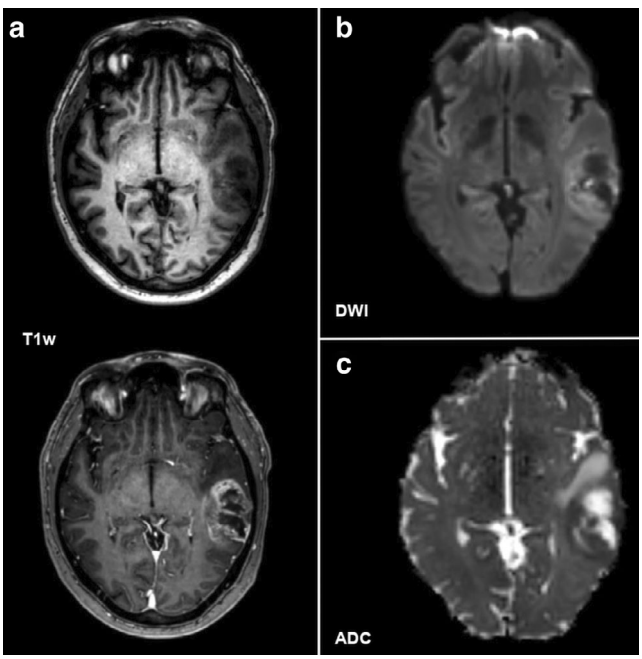


FIGURE 5: Diffusion restriction in a 45-year-old female patient with a left temporal high-grade glioma (HGG) that showed contrast enhancement on T1-weighted imaging (a; axial non-contrast and contrast-enhanced images). On diffusion-weighted imaging (DWI, $b = 1000$ s/mm^2), the borders of the lesion that primarily overlap with the contrast-enhancing tumor parts show high signal intensity (b) that spatially corresponded to areas with a signal drop on apparent diffusion coefficient (ADC) maps (c), indicating restricted diffusion most probably due to focal high cellularity of the glioma.

Specifically, ADC values were successfully applied to differentiate between LGG and HGG, with a summarized sensitivity and specificity of 0.85 and 0.80, respectively, and a summary ROC-based AUC of 0.90 as derived from a meta-analysis consisting of 15 studies.[71] Also, ADC values were significantly higher in IDH1-mutated gliomas than in IDH1-wild-type gliomas.[72] Furthermore, ADC was associated with different histologic and genetic types of WHO grade II-III diffuse gliomas, considering both the 2007 and 2016 WHO classifications, especially for 1p/19q co-deletion and IDH1 mutation status.[73] ADC values were also successfully used in a multi-center study to predict the EGFR amplification status of IDH-wild-type WHO grade II-III gliomas.[74] Specifically, lower mean ADC and the lower 5th percentile of ADC values were potentially useful imaging biomarkers for EGFR amplification in IDH-wild-type glioma.[74] Previously, the assessment of ADC values in different parenchyma and brain tumor regions has also been considered, and for patients with IDH-mutated tumors, ADC values were significantly higher in tumor tissue than in marginal areas of the tumor, while there were no significant differences in terms of ADC values between tumor tissue and marginal areas of the tumor for patients with IDH-wild-type tumors.[75] The assessment of ADC values in H3 K27M histone-mutant diffuse midline glioma, a recently classified neoplasm, revealed that mean ADC was $0.84 \pm 0.15 \times 10^{-3}$ mm^2/s.[76] Another study also addressed the diffuse midline glioma H3 K27-mutant, and concluded that lower ADC values in non-enhancing areas may be related to the normal expression of ATRX.[77]

It has been demonstrated that maximal and/or mean FA values are usually significantly higher in HGG, which may be due not only to infiltration, but also to disruption of fibers compared to LGG with mainly infiltration without disruption.[78] Yet, the opposite has been reported for WHO grade II and grade III gliomas as well, which was mostly because FA values were dominated by tumor infiltration that caused disruption of the neuronal, axonal, and glial microstructure rather than by changes due to abnormal cellularity.[79] In addition to differentiating glioma with respect to the WHO grading, studies have investigated the ability to discriminate between tumors according to IDH mutation status, and maximal FA and the ratio of maximal FA (maximal FA divided by the contralateral normal FA) were significantly different between oligodendroglial tumors with IDH mutations and those without mutations, yielding areas under the curve (AUCs) of 0.79 and 0.82, respectively.[80] Moreover, a positive association was observed between IDH1 status and MD in a cohort of patients with HGG.[81] Similarly, whole-tumor histograms, as well as texture analysis of FA maps, enabled prediction of the IDH1-mutation and 1p/19q-codeletion status in patients with WHO grade II gliomas.[82] In addition, evaluation of FA in the peritumoral region may enable conclusions to be drawn at baseline about potential spatial recurrence patterns.[83]

15222586, 2023, 6, Downloaded from https://onlinelibrary.wiley.com/doi/10.1002/jmri.28662 by Imperial College London, Wiley Online Library on [24/05/2023]. See the Terms and Conditions (https://onlinelibrary.wiley.com/terms-and-conditions) on Wiley Online Library for rules of use; OA articles are governed by the applicable Creative Commons License

More advanced techniques, such as DKI and IVIM imaging, have been applied to preoperative imaging in neuro-oncology. Specifically, MK values derived from DKI were used for grading, and it has been shown that MK values increased with higher glioma malignancy.[84] Furthermore, it has been demonstrated that axial kurtosis and radial kurtosis values were also increased in cases of HGG vs. LGG, outlining the application of MK for grading (WHO grades II-IV) and predicting Ki-67 as a metric related to cellularity.[85] Moreover, another metric used was MK, a parameter derived from fast kurtosis imaging, which showed increased values in HGG compared to LGG.[86] Another possible application of DKI in the setting of integrated glioma diagnosis is the prediction of the IDH mutation status based on the intrinsic tumoral heterogeneity as expressed by variant intravoxel kurtosis features.[87] Similarly, IVIM imaging has shown great potential, since it has demonstrated the ability to differentiate between HGG and LGG, and to support the prediction of survival for newly diagnosed HGG and the treatment outcome in the course of therapy.[88,89]

VALIDATION. The application of diffusion MRI in neuro-oncological imaging may represent a promising technique to assess tissue microstructure in the presence of glioma. However, there are multiple sequences and analysis techniques available that may not be feasible for each center and MRI system used. One shortcoming is that most centers use a single-shot EPI method for diffusion sequences because of its short acquisition times. However, this approach provides limited spatial resolution and can be adversely affected by susceptibility artifacts that can mislead qualitative and quantitative analysis, notably at tissue interfaces. Moreover, EPI-based eddy currents can create image distortions that confound diffusion parameter evaluation. Furthermore, motion artifacts are a relevant problem for sequences with long acquisition times, including diffusion MRI.

While basic diffusion-weighted imaging (DWI) is usually acquired rapidly, multi-directional DTI acquisitions can take several minutes and therefore are particularly prone to head motion artifacts. Several processing tools may be used to correct residual motion artifacts in DTI results, and a combined approach using prospective and retrospective motion-correction techniques could facilitate overall distortion correction. In particular, DWI is also prone to perfusion effects from water movement in the capillary network, which can possibly overestimate ADC in highly vascular tumors. Conversely, diffusion and perfusion effects can be separated and specifically used for glioma imaging with the IVIM technique.

SUMMARY. For preoperative imaging, DWI is among the most frequently used sequences besides conventional structural imaging. Particularly, basic measurements (i.e., ADC and FA) have been investigated in detail for the differentiation between certain glioma entities and, more recently, also to predict different glioma molecular subtypes. However, mostly EPI-based and DTI techniques have been applied, while more advanced methods such as DKI or IVIM imaging have become increasingly available for the clinical setting and can provide more detailed insights into tissue microstructure.

Vessel Imaging

OVERVIEW. ***MR Angiography.*** The principal method used for MRA is time-of-flight (TOF) angiography, also known as inflow angiography, which does not require GBCA administration, but instead visualizes arteries using the magnetically unsaturated spins of flowing blood, which has more signal than the surrounding tissue.

Vessel-Architectural Imaging. By acquiring a combined GRE and SE EPI sequence during an intravenous GBCA injection, the average vessel calibers can be estimated in glioma by so-called vessel-architectural imaging (VAI), sometimes also referred to as vessel size imaging.[90] The highly susceptibility-sensitive GRE signal is sensitive to blood vessels of all calibers, whereas SE is predominantly sensitive to microscopic vessels or capillaries (radius < 10 μm).[91] This phenomenon is further exploited in VAI to provide further insight into vessel size and type (Fig. 6). The differing sensitivity to the susceptibility effect of SE and gradient-echo readouts creates a relative and temporal shift in the shape and peak position of the GBCA-induced signal curves when plotted.[92]

CLINICAL APPLICATION. ***MR Angiography.*** Limited studies have reported attempts to assess glioma based on MRA techniques in humans. These are small pilot or older studies, none of which includes histological differentiation.

In line with works by Kadota et al that demonstrated the value of TOF to identify pathological neovascularization,[93] Radbruch et al presented a limited 7T pilot, which showed that high-resolution (0.3 × 0.3 × 0.4 mm) TOF made arterial vessels not only visible, but also quantifiable, with more and denser vessels in glioblastoma compared to normal tissue.[94] A more recent study found that a new analysis method that measures local vessel orientation angles can help differentiate normal from abnormal tumor vessels.[95]

MRA studies are especially driven by their utility for neurosurgical planning, eg, to delineate lenticulostriate arteries. One smaller study showed that hypervascularization of glioblastoma with contrast-enhanced MR angiography (CE-MRA)[96] is an excellent marker of reduced OS.

Vessel-Architectural Imaging. Several VAI studies with a medium-sized patient group (50–100 participants) have demonstrated successful differentiation by brain tumor histology in patients with glioma. VAI was successfully applied to

15222586, 2023, 6, Downloaded from https://onlinelibrary.wiley.com/doi/10.1002/jmri.28662 by Imperial College London, Wiley Online Library on [24/05/2023]. See the Terms and Conditions (https://onlinelibrary.wiley.com/terms-and-conditions) on Wiley Online Library for rules of use; OA articles are governed by the applicable Creative Commons License

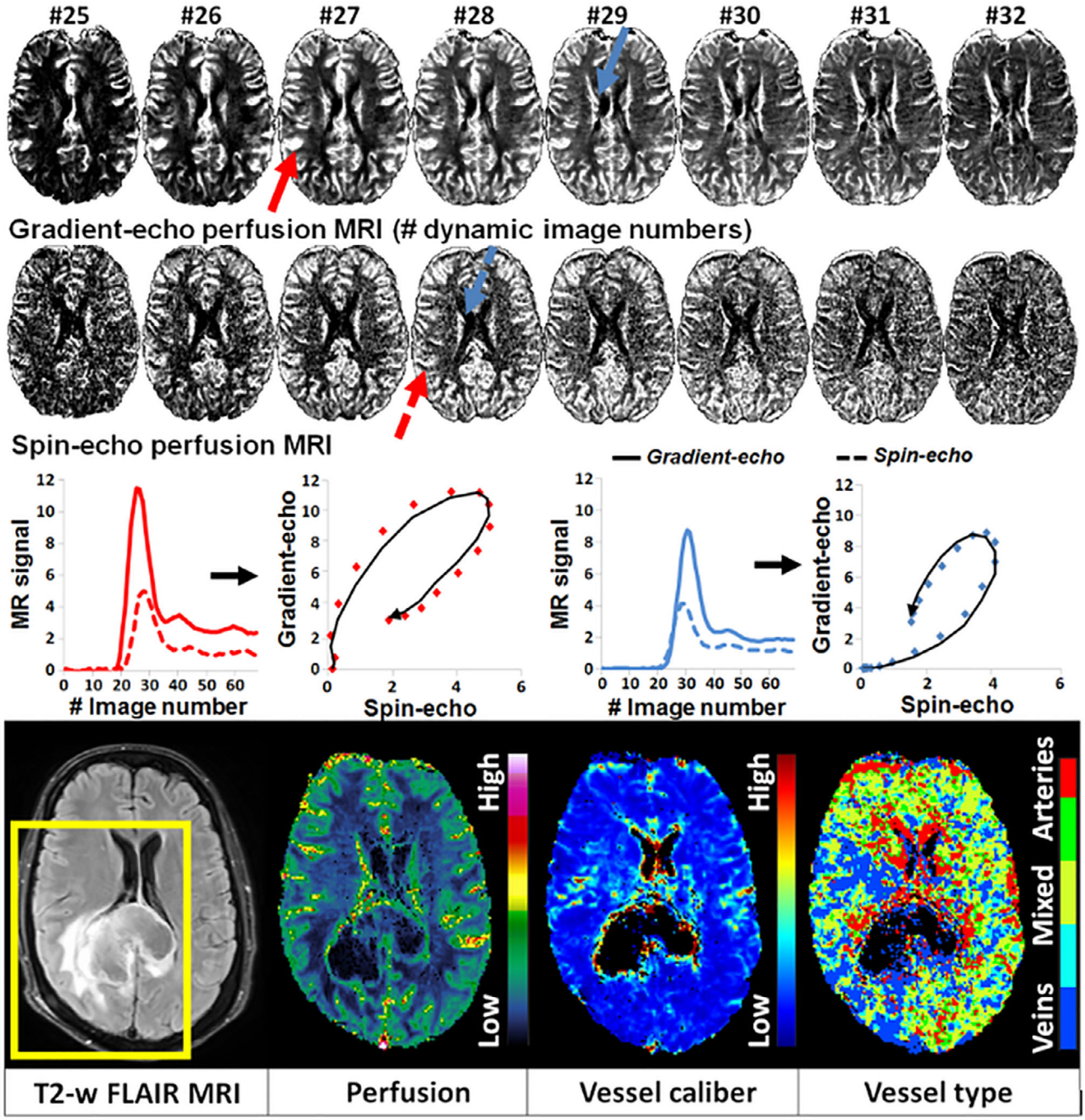


FIGURE 6: Perfusion MRI and vessel-architectural imaging (VAI). Merging two perfusion readouts (gradient- and spin-echo MRI) creates unique signal curve "loops" that scale with vessel calibers (slope) and vessel type (loop direction). Note the impaired, venous-like dominance of the peri-tumoral area (yellow box) on the vessel type map of a glioblastoma not observed on other images. Adapted from Emblem et al, Nature Medicine 2003.[92]

examine differences in vasculature between untreated glioma types according to the 2016 WHO classification.[97] This also included differentiation by IDH mutation based on VAI parameters at an AUC of 0.782.[98] Notably, no studies exist using the WHO 2021 classification. Moreover, VAI-associated biomarkers are valuable in the assessment of the heterogeneity of the glioma microvasculature that arises from the angiogenic activity of these tumors. VAI maps proved helpful for the delineation of glioma from peripheral edema.[99] Stadlbauer et al suggested using vascular-induced peak shift and the microvessel type indicator to allow early neovascularization detection, while curvature might be a marker for the severity of vasogenic edema.[100]

VALIDATION. ***MR Angiography.*** Different studies have suggested that MR angiography has substituted conventional angiography for the assessment of intracranial vessels.[101] TOF angiography (i.e., the main MR angiography technique), when used on clinical scanners (≤3T), is less accurate than

15222586, 2023, 6, Downloaded from https://onlinelibrary.wiley.com/doi/10.1002/jmri.28662 by Imperial College London, Wiley Online Library on [24/05/2023]. See the Terms and Conditions (https://onlinelibrary.wiley.com/terms-and-conditions) on Wiley Online Library for rules of use; OA articles are governed by the applicable Creative Commons License

contrast-enhanced MRA (CEMRA) and digital subtraction angiography (DSA).[102] However, DSA and CEMRA are invasive, or, at best, require contrast agents that trigger adverse effects. Ultra-high magnetic field (i.e., 7T) scanners have opened the door to a substantial improvement in the quality and contrast of the structures of interest in TOF angiography. Nevertheless, these advances are far from clinical application due to the limited availability of 7T scanners and artifacts due to magnetic field inhomogeneity.

Vessel-Architectural Imaging. Outside a few major research institutions, VAI is not yet clinically available for patients with glioma, even though both vessel size and perfusion parameters could be derived simultaneously from the same dataset. This is mainly due to a lack of standardization of optimal imaging parameters and intricate post-processing routines requiring dedicated analysis software, and special expertise. Finally, based on the complex biology and overlapping distribution of tumor-vessel calibers across different brain tumor types, quantitative assessments using a cut-off value for vessel size may not discriminate between tumor types or treatment outcomes. Instead, relative measures of vessel size are most often used, which further increases the complexity of the technique. Taken together, to date, only a relatively small number of clinical studies have been performed and with limited (N < 50) and diverse patient cohorts.

SUMMARY. ***MR Angiography.*** TOF angiography, the most commonly used method for MR angiography, has advantages over other established conventional angiography modalities, such as CEMRA or DSA, as it is noninvasive and does not require external contrast agents. However, on clinical scanners, TOF angiography lacks the accuracy of conventional modalities, and its use in glioma analysis is currently limited to very specific studies mainly related to surgical planning or analysis of the vascular architecture from a morphological point of view.

Vessel-Architectural Imaging. Because angiogenesis is a hallmark of cancer, assessment of the vasculature by VAI constitutes an attractive tool for diagnosis and monitoring. However, the technique still suffers from a lack of clinical validation by cross-vendor repeatability and reliability tests. With a continued focus on implementation guidelines and automatic analysis pipelines, the utility and availability of VAI may greatly improve even outside the research community.

Relaxometry and MR Fingerprinting (MRF)

OVERVIEW. Quantitative mapping of T1 and T2 relaxation times offers more specific and robust characterization of glioma compared to conventional structural imaging techniques. Early pulse sequences involved changing one acquisition parameter at a time and, while inversion recovery mapping of T1 and SE mapping of T2 remain gold-standard techniques, they are prohibitively time-consuming for clinical use.[103] Acquisition times can be greatly reduced using simultaneous multiparametric mapping techniques, such as Magnetic Resonance Image Compilation (MAGiC),[104] and Magnetic Resonance Fingerprinting (MRF).[105]

In MRF, a pulse sequence with pseudo-randomly varying acquisition parameters (eg, flip angle and repetition time) results in temporally varying measured signals, termed fingerprints, for each voxel. Fingerprints are dictated by multiple relaxation mechanisms (eg, T1, T2), and a dictionary can be generated by pre-calculating predicted combinations of parameter values using simulations and Bloch equations. The acquired fingerprints are matched with the dictionary entries to deduce voxel-wise parameter values and reconstruct quantitative maps (Fig. 7).

CLINICAL APPLICATION. ***Biological Relevance of T1 and T2 Mapping.*** T1 and T2 relaxation times of tissue are influenced by the number of lipids, proteins, macromolecules, and paramagnetic materials present, as well as the local water content, microstructure, and cellularity. The T1 and T2 relaxation times of tumors have been found to be longer than that of surrounding healthy tissue,[107–109] with contrast thought to be mainly driven by increased hydration in the form of intra-tumoral edema,[110] which occurs due to leaky vessels as a consequence of neovascularization.

Further classification or grading of gliomas has been investigated but is less straightforward. In a 2D fingerprinting study by Badve et al, solid tumor regions of LGG and

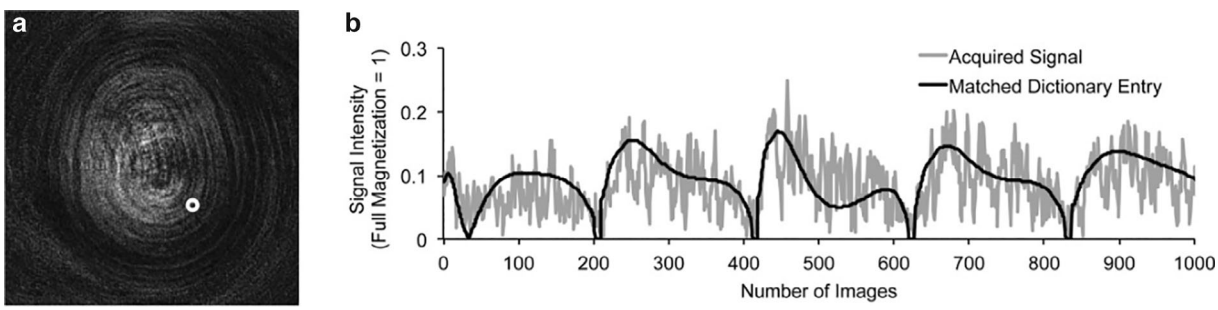


FIGURE 7: Schematic depicting an example of a fingerprint (a) with its corresponding best-acquired signal and matched dictionary entry (b). Reproduced with permission from Jiang et al Magn Reson Med 2015.[106]

15222586, 2023, 6, Downloaded from https://onlinelibrary.wiley.com/doi/10.1002/jmri.28662 by Imperial College London, Wiley Online Library on [24/05/2023]. See the Terms and Conditions (https://onlinelibrary.wiley.com/terms-and-conditions) on Wiley Online Library for rules of use; OA articles are governed by the applicable Creative Commons License

metastases were significantly different, but overlap in the range between tissues meant it was not possible to distinguish between LGG and HGG based on average relaxation times.[107]

That study concluded that relaxation times in glioma were mainly driven by cellularity type and the common glial origin, meaning tumor grades could not be differentiated based on mean values alone. Further radiomics analysis of the same quantitative fingerprinting dataset revealed significant differences between metastasis, LGGs, and HGGs.[111] A significant correlation has also been found between lower T1 entropy (representing lower heterogeneity) and survival.[111] In a small study including 14 children and 9 young adults (ages 1–34), significant differences were found in mean MRF-derived T1/T2 values between 19 LGGs and 4 HGGs, and between tumor and contralateral white matter.[108]

More recent studies have addressed the role of multi-echo SE T2 mapping in IDH mutation status of adult LGGs

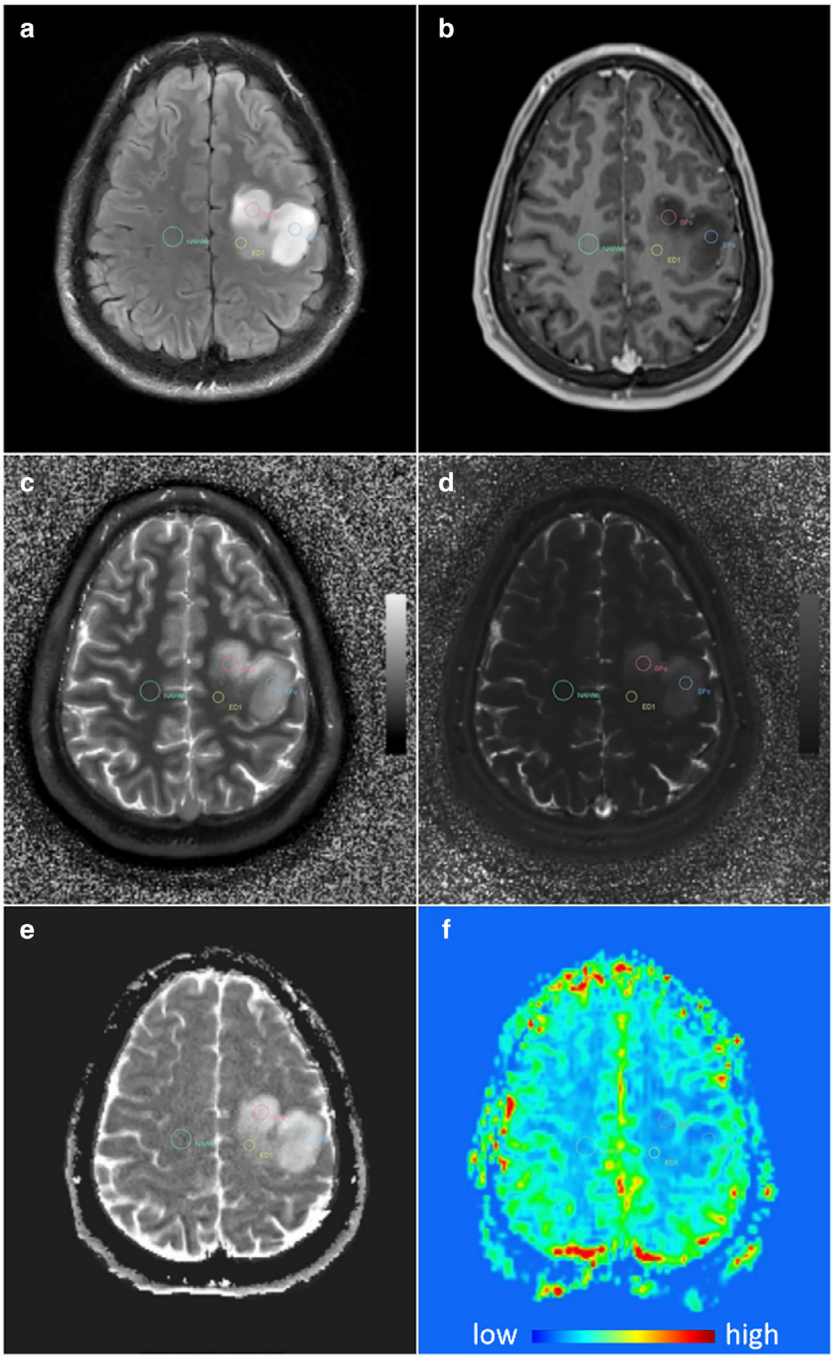


FIGURE 8: Quantitative maps derived from MRF in an astrocytoma, IDH-mutant, show increased T1 and T2 values within the tumor mass. The MRF T1 map (c) and T2 map (d) are compared to FLAIR (a), T1w contrast-enhanced MRI (b), an ADC map (e), and perfusion-weighted imaging (f). Reproduced from Springer et al 2022 under CC license.[112]

15222586, 2023, 6, Downloaded from https://onlinelibrary.wiley.com/doi/10.1002/jmri.28662 by Imperial College London, Wiley Online Library on [24/05/2023]. See the Terms and Conditions (https://onlinelibrary.wiley.com/terms-and-conditions) on Wiley Online Library for rules of use; OA articles are governed by the applicable Creative Commons License

and showed an increase in T2 in IDH-mutant glioma compared to IDH-wildtype glioma.[109] This was also observed in an MRF study, which showed an increase in T1 values in the solid component of IDH mutant glioma, compared to wildtype.[112] An example of these findings is displayed in Fig. 8.

Quantitative imaging could also provide insight into the extent of non-enhancing tumor invasion into peritumoral edema. Quantitative MAGiC mapping found T1 and T2 relaxation times could detect tumor invasion and the peritumoral regions of T1 maps showed post-contrast enhancement, neither of which was visible on conventional imaging.[113,114] Variable flip angle T1 mapping and multi-echo SE T2 mapping have yielded similar results,[115] suggesting a broader infiltration can be identified using postcontrast quantitative mapping. Edema surrounding LGGs was found to have lower mean T1 times mapped by MRF than the edema around HGGs,[107] but postcontrast MRF studies have not yet been reported.

VALIDATION. MRF is a recent technique that holds great promise in introducing rapid quantitative T1 and T2 mapping into the clinic; however, only a small number of clinical studies have been performed. These studies have had limited patient cohort numbers, with an uneven distribution of glioma grades and types, as well as different methods for tumor segmentation and data analyses. The majority of MRF studies have been implemented using a 2D sequence. However, a proof-of-concept study evaluated a 3D fingerprinting-style, quantitative, transient-state imaging (QTI) sequence in nine glioma patients (grades 2–4) with varying treatment histories, and showed the feasibility of 3D acquisitions in glioma, with a whole-brain acquisition time under 7 minutes.[116] Finally, the repeatability and reliability of MRF in a clinical environment need to be further validated to confirm the positive results in healthy brains.[117]

SUMMARY. Still in its infancy, MRF promises to be a technique that will aid in the characterization and delineation of brain tumors, making quantitative T1 and T2 imaging acquisitions rapid and ready for use in a clinical environment.[118] Larger validation studies are expected in the near future as MRF becomes more widely available.

Overview: Level of Clinical Validation

Discussion

In this review, a working group of the GliMR COST action has summarized the evidence for clinical use of advanced MRI for preoperative glioma characterization.

The most frequently used advanced-MRI sequence is DWI. The likely reasons—the ease of implementation, wide availability, and frequent use in other pathologies—might be more important for the widespread use than DWI's diagnostic potential. Notably, advanced diffusion sequences, like IVIM and DKI, are used only marginally in glioma due to their lower availability and more difficult processing and interpretation.

In contrast, DSC is an exemplary case of accelerating the clinical translation of advanced MRI. DSC involves contrast-agent injection, input function delineation, tracer-kinetic modeling, and value normalization. Despite its complexity, DSC is commonly used in glioma imaging[14] owing mainly to the extensive work invested in DSC validation. This work culminated recently by introducing consensus recommendations,[18] which provide clear instructions on the measurement and evaluation processes and is backed up by robust validation. Such recommendations constitute an important step toward clinical acceptance and are missing for nearly all other advanced MRI techniques.

The level of clinical validation also depends on more general determinants. Glioma is a relatively rare disease, making it difficult to collect enough data for statistically robust assessments. The Brain Tumor Segmentation (BraTS) repository initiative partly addresses this by collecting multi-institutional pre-operative multi-parametric MRI scans of patients with glioma.[119] Still, regardless of the level of good-quality evidence, lack of widespread use may boil down to something as simple as limited demand and early adoption from key practitioners due to preference, education, and above all awareness. With increasing demand, shorter time to read exams, and reduced hospital budgets, it may be difficult for the radiologist or end user to stay up to date with the wide range of available methods, or find the time and resources to lead the clinical implementation. For any new technique, adaptation and priority of use will be weighed against the cost and resources of the exam, its associated clinical workup, and the initial implementation and training of bioengineers and neuroradiologists. In practice, this may be a question of healthcare reimbursement policies and insurance coverage, which usually do not include techniques that are not part of the guidelines. Several initiatives are trying to make up for this difference by reviewing the abilities of advanced MRI[6]; building networks of professionals in glioma imaging, providing educational resources and processing tools for advanced MRI, and connecting with other professionals in neuro-oncology as in GliMR[10]; working on providing open source software for data analysis like the Open Science Initiative For Perfusion Imaging (OSIPI)[120]; or seeking to improve the practical value of quantitative imaging biomarkers as the Quantitative Imaging Biomarkers Alliances (QIBA) does.[121]

Despite the promise of improved diagnostic efficiency of the new imaging biomarkers, clinical translation will need to respect the cost–benefit ratio of its use and the patient's health status. This translates to keeping the acquisition duration mostly unchanged and replacing old sequences with newer ones only if the added value compensates for the hurdles associated with introducing new techniques. For example, while DCE measures both the permeability of the BBB

15222586, 2023, 6, Downloaded from https://onlinelibrary.wiley.com/doi/10.1002/jmri.28662 by Imperial College London, Wiley Online Library on [24/05/2023]. See the Terms and Conditions (https://onlinelibrary.wiley.com/terms-and-conditions) on Wiley Online Library for rules of use; OA articles are governed by the applicable Creative Commons License

and vascularization and is potentially more useful than DSC, it is not straightforward to measure both sequences within a single session. Therefore, DSC is currently prioritized as a quicker and more robust technique that already has well-established guidelines and a much higher level of validation. Overall, GBCA use in gliomas is likely to be reduced in the future due to added burden to costs, logistics, and patient discomfort burdens, as well as safety issues raised by both American and European pharmacological safety agencies. ASL,[57] BBB-ASL,[122] and machine-learning-based techniques are on a good path to complement and maybe eventually replace DSC, DCE, and post-contrast T1-weighted scans, respectively, in many glioma patients and especially children. Although MRF has not been validated, its promise to provide fully quantitative measurements of relaxation times could obviate the conventional protocol and thus make space for other advanced sequences like VSI, CEST, or MRS.

Even when advanced diagnostic tools are implemented and available to the end user, their clinical use is challenged by an inherent paradox. As imaging techniques become more advanced, so do their resulting imaging biomarkers, where any metric will move away from a simple binary (yes/no) or cutoff (above/below) value for characterization. With a higher-level technique, the complex biology and function of cancer will arguably be assessed in a more accurate and unique way, but at the cost of more difficult interpretations. Multi-parametric assessment combining several advanced MRI techniques may also further improve glioma characterization and reduce the bias of any single technique toward certain biological or functional properties of the tissue. However, a multi-parametric approach will also add to the complexity of the analysis. As a result, in a busy practice there may be no time, nor may it be technically feasible, for radiologists to process this data. For advanced imaging methods to be widely adopted, a strong focus is required on translating clinically ready technology into commercial software directly embedded in the hospital-wide picture archiving and communication system (PACS). This will allow for standardization and start-to-end automatic pipelines as an alternative to laborious and user-dependent alternatives.

In conclusion, effective treatment of gliomas is still an unmet clinical need that is, in part, reflected by their wide-ranging intra- and inter-individual biological heterogeneity. Targeted therapy, which has demonstrated promising results in other cancers, has largely failed in gliomas. To address this challenge, the advanced imaging techniques discussed in this review hold the potential to support better clinical decisions for tumor characterization and subsequent treatment. By focusing on what these techniques are currently missing to advance their clinical readiness level, the imaging community can help make advanced MRI for glioma diagnosis and therapy clinically available, personalized, and effective.

Acknowledgments

We want to thank Rosa Ayesa Arriola, Martin Barak, Paula Croal, Philip De Witt Hamer, Vasileios K. Katsaros, Mary Pelechrini, Zahra Shams, Danai-Eleni Stefanou, Ioannis John Toliopoulos, and Hana Valekova for their assistance with earlier versions of this manuscript. This review was funded by grants from the following agencies: Dutch Research Council (NWO), Veni project numbers 91619121 and 16862, VICI project number 016.160.351; Wellcome Trust 2022-24, 203148/A/16/Z; Spanish Ministry of Science and Innovation (grant: PI18/00084), Spanish State Research Agency, Subprogram for Knowledge Generation (PROGRESS, No PID2021-127110OA-I00). Austrian Science Funds (FWF) projects KLI 646 and 1089; a 2021 Comprehensive Cancer Center grant of the Medical University of Vienna; The Turkish Directorate of Strategy and Budget under the TAM Project number 2007K12-873; INTER-EXCELLENCE, subprogram INTER-COST of the Ministry of Education, Youth and Sports CZ, Grant No. LTC20027; TUBITAK 1003 grant 216S432; European Research Agency, Marie Sklodowska Curie Fellowship, Horizon 2020; NIH/NCI U01 CA176110, NIH/NCI R01 CA264992, NIH/NCI CA255123; HollandPTC-Varian grant ID: 2018017; European Union's Horizon 2020 Programme: ERC Grant Agreement No. 758657-ImPRESS; South-Eastern Norway Regional Health Authority Grant Agreements No. 2016102, 2017073, 2013069; the Norwegian Cancer Society and the Research Council of Norway FRIPRO Grant Agreements No. 261984, 303249; the MS Society of the United Kingdom (grant: 125); and the American Heart Association (Grant: 826254). This publication is part of the COST Action CA18206 Glioma MR Imaging 2.0, supported by COST (European Cooperation in Science and Technology), www.cost.eu www.glimr.eu.

References

1. Miller KD, Ostrom QT, Kruchko C, et al. Brain and other central nervous system tumor statistics, 2021. CA Cancer J Clin 2021;71:381-406.
2. Louis DN, Perry A, Wesseling P, et al. The 2021 WHO classification of tumors of the central nervous system: A summary. Neuro Oncol 2021; 23:1231-1251.
3. Horbinski C, Berger T, Packer RJ, Wen PY. Clinical implications of the 2021 edition of the WHO classification of central nervous system tumours. Nat Rev Neurol 2022;18:515-529.
4. Louis DN, Perry A, Reifenberger G, et al. The 2016 World Health Organization classification of tumors of the central nervous system: A summary. Acta Neuropathol 2016;131:803-820.
5. Ellingson BM, Bendszus M, Boxerman J, et al. Consensus recommendations for a standardized brain tumor imaging protocol in clinical trials. Neuro Oncol 2015;17:1188-1198.
6. Smits M. MRI biomarkers in neuro-oncology. Nat Rev Neurol 2021;17: 486-500.

15222586, 2023, 6, Downloaded from https://onlinelibrary.wiley.com/doi/10.1002/jmri.28662 by Imperial College London, Wiley Online Library on [24/05/2023]. See the Terms and Conditions (https://onlinelibrary.wiley.com/terms-and-conditions) on Wiley Online Library for rules of use; OA articles are governed by the applicable Creative Commons License

7. Villanueva-Meyer JE, Mabray MC, Cha S. Current clinical brain tumor imaging. Neurosurgery 2017;81:397-415.

8. Eckel-Passow JE, Lachance DH, Molinaro AM, et al. Glioma groups based on 1p/19q, IDH, and TERT promoter mutations in tumors. N Engl J Med 2015;372:2499-2508.

9. Wijnenga MMJ, French PJ, Dubbink HJ, et al. The impact of surgery in molecularly defined low-grade glioma: An integrated clinical, radiological, and molecular analysis. Neuro Oncol 2018;20:103-112.

10. Clement P, Booth T, Borovečki F, et al. GliMR: Cross-border collaborations to promote advanced MRI biomarkers for glioma. J Med Biol Eng 2020;41:1-11.

11. Romeo V, Stanzione A, Ugga L, et al. A critical appraisal of the quality of glioma imaging guidelines using the AGREE II tool: A EuroAIM initiative. Front Oncol 2019;9:472.

12. deSouza NM, van der Lugt A, Deroose CM, et al. Standardised lesion segmentation for imaging biomarker quantitation: A consensus recommendation from ESR and EORTC. Insights Imaging 2022;13:159.

13. O'Connor JPB, Aboagye EO, Adams JE, et al. Imaging biomarker roadmap for cancer studies. Nat Rev Clin Oncol 2017;14:169-186.

14. Manfrini E, Smits M, Thust S, et al. From research to clinical practice: A European neuroradiological survey on quantitative advanced MRI implementation. Eur Radiol 2021;31:6334-6341.

15. Donahue KM, Krouwer HG, Rand SD, et al. Utility of simultaneously acquired gradient-echo and spin-echo cerebral blood volume and morphology maps in brain tumor patients. Magn Reson Med 2000;43:845-853.

16. Boxerman JL, Schmainda KM, Weisskoff RM. Relative cerebral blood volume maps corrected for contrast agent extravasation significantly correlate with glioma tumor grade, whereas uncorrected maps do not. AJNR Am J Neuroradiol 2006;27:859-867.

17. Paulson ES, Schmainda KM. Comparison of dynamic susceptibility-weighted contrast-enhanced MR methods: Recommendations for measuring relative cerebral blood volume in brain tumors. Radiology 2008;249:601-613.

18. Boxerman JL, Quarles CC, Hu LS, et al. Consensus recommendations for a dynamic susceptibility contrast MRI protocol for use in high-grade gliomas. Neuro Oncol 2020;22:1262-1275.

19. Quarles CC, Ward BD, Schmainda KM. Improving the reliability of obtaining tumor hemodynamic parameters in the presence of contrast agent extravasation. Magn Reson Med 2005;53:1307-1316.

20. Bjornerud A, Sorensen AG, Mouridsen K, Emblem KE. T1- and T2*-dominant extravasation correction in DSC-MRI: Part I--theoretical considerations and implications for assessment of tumor hemodynamic properties. J Cereb Blood Flow Metab 2011;31:2041-2053.

21. Leu K, Boxerman JL, Cloughesy TF, et al. Improved leakage correction for single-Echo dynamic susceptibility contrast perfusion MRI estimates of relative cerebral blood volume in high-grade gliomas by accounting for bidirectional contrast agent exchange. AJNR Am J Neuroradiol 2016;37:1440-1446.

22. Sugahara T, Korogi Y, Kochi M, et al. Correlation of MR imaging-determined cerebral blood volume maps with histologic and angiographic determination of vascularity of gliomas. AJR Am J Roentgenol 1998;171:1479-1486.

23. Lev MH, Ozsunar Y, Henson JW, et al. Glial tumor grading and outcome prediction using dynamic spin-echo MR susceptibility mapping compared with conventional contrast-enhanced MR: Confounding effect of elevated rCBV of oligodendrogliomas [corrected]. AJNR Am J Neuroradiol 2004;25:214-221.

24. Schmainda KM, Rand SD, Joseph AM, et al. Characterization of a first-pass gradient-echo spin-echo method to predict brain tumor grade and angiogenesis. AJNR Am J Neuroradiol 2004;25:1524-1532.

25. McCullough BJ, Ader V, Aguedan B, et al. Preoperative relative cerebral blood volume analysis in gliomas predicts survival and mitigates risk of biopsy sampling error. J Neurooncol 2018;136:181-188.

26. Soliman RK, Gamal SA, Essa A-HA, Othman MH. Preoperative grading of glioma using dynamic susceptibility contrast MRI: Relative cerebral blood volume analysis of intra-tumoural and peri-tumoural tissue. Clin Neurol Neurosurg 2018;167:86-92.

27. Juan-Albarracín J, Fuster-Garcia E, Pérez-Girbés A, et al. Glioblastoma: Vascular habitats detected at preoperative dynamic susceptibility-weighted contrast-enhanced perfusion MR imaging predict survival. Radiology 2018;287:944-954.

28. Maeda M, Itoh S, Kimura H, et al. Tumor vascularity in the brain: Evaluation with dynamic susceptibility-contrast MR imaging. Radiology 1993;189:233-238.

29. Connelly JM, Prah MA, Santos-Pinheiro F, Mueller W, Cochran E, Schmainda KM. Magnetic resonance imaging mapping of brain tumor burden: Clinical implications for neurosurgical management: Case report. Neurosurg Open 2021;2:okab029.

30. Parker NR, Khong P, Parkinson JF, Howell VM, Wheeler HR. Molecular heterogeneity in glioblastoma: Potential clinical implications. Front Oncol 2015;5:55.

31. Lu J, Li X, Li H. Perfusion parameters derived from MRI for preoperative prediction of IDH mutation and MGMT promoter methylation status in glioblastomas. Magn Reson Imaging 2021;83:189-195.

32. Pedeutour-Braccini Z, Burel-Vandenbos F, Gozé C, et al. Microfoci of malignant progression in diffuse low-grade gliomas: Towards the creation of an intermediate grade in glioma classification? Virchows Arch 2015;466:433-444.

33. Patel P, Baradaran H, Delgado D, et al. MR perfusion-weighted imaging in the evaluation of high-grade gliomas after treatment: A systematic review and meta-analysis. Neuro Oncol 2017;19:118-127.

34. Prah MA, Stufflebeam SM, Paulson ES, et al. Repeatability of standardized and normalized relative CBV in patients with newly diagnosed glioblastoma. AJNR Am J Neuroradiol 2015;36:1654-1661.

35. Schmainda KM, Prah MA, Marques H, Kim E, Barboriak DP, Boxerman JL. Value of dynamic contrast perfusion MRI to predict early response to bevacizumab in newly diagnosed glioblastoma: Results from ACRIN 6686 multicenter trial. Neuro Oncol 2021;23:314-323.

36. Schmainda KM, Prah MA, Rand SD, et al. Multisite concordance of DSC-MRI analysis for brain tumors: Results of a National Cancer Institute Quantitative Imaging Network Collaborative Project. AJNR Am J Neuroradiol 2018;39:1008-1016.

37. Hu LS, Eschbacher JM, Heiserman JE, et al. Reevaluating the imaging definition of tumor progression: Perfusion MRI quantifies recurrent glioblastoma tumor fraction, pseudoprogression, and radiation necrosis to predict survival. Neuro Oncol 2012;14:919-930.

38. Prah MA, Al-Gizawiy MM, Mueller WM, et al. Spatial discrimination of glioblastoma and treatment effect with histologically-validated perfusion and diffusion magnetic resonance imaging metrics. J Neurooncol 2018;136:13-21.

39. Hu LS, Kelm Z, Korfiatis P, et al. Impact of software modeling on the accuracy of perfusion MRI in glioma. AJNR Am J Neuroradiol 2015;36:2242-2249.

40. Milchenko MV, Rajderkar D, LaMontagne P, et al. Comparison of perfusion- and diffusion-weighted imaging parameters in brain tumor studies processed using different software platforms. Acad Radiol 2014;21:1294-1303.

41. Schmainda KM, Zhang Z, Prah M, et al. Dynamic susceptibility contrast MRI measures of relative cerebral blood volume as a prognostic marker for overall survival in recurrent glioblastoma: Results from the ACRIN 6677/RTOG 0625 multicenter trial. Neuro Oncol 2015;17:1148-1156.

42. Gerstner ER, Zhang Z, Fink JR, et al. ACRIN 6684: Assessment of tumor hypoxia in newly diagnosed glioblastoma using 18F-FMISO PET and MRI. Clin Cancer Res 2016;22:5079-5086.

43. Stokes AM, Skinner JT, Quarles CC. Assessment of a combined spin- and gradient-echo (SAGE) DSC-MRI method for preclinical neuroimaging. Magn Reson Imaging 2014;32:1181-1190.

15222586, 2023, 6, Downloaded from https://onlinelibrary.wiley.com/doi/10.1002/jmri.28662 by Imperial College London, Wiley Online Library on [24/05/2023]. See the Terms and Conditions (https://onlinelibrary.wiley.com/terms-and-conditions) on Wiley Online Library for rules of use; OA articles are governed by the applicable Creative Commons License

44. Skinner JT, Robison RK, Elder CP, Newton AT, Damon BM, Quarles CC. Evaluation of a multiple spin- and gradient-echo (SAGE) EPI acquisition with SENSE acceleration: Applications for perfusion imaging in and outside the brain. Magn Reson Imaging 2014;32:1171-1180.

45. Khalifa F, Soliman A, El-Baz A, et al. Models and methods for analyzing DCE-MRI: A review. Med Phys 2014;41:124301.

46. Tofts PS, Brix G, Buckley DL, et al. Estimating kinetic parameters from dynamic contrast-enhanced t1-weighted MRI of a diffusable tracer: Standardized quantities and symbols. J Magn Reson Imaging 1999;10:223-232.

47. Yun TJ, Park C-K, Kim TM, et al. Glioblastoma treated with concurrent radiation therapy and temozolomide chemotherapy: Differentiation of true progression from pseudoprogression with quantitative dynamic contrast-enhanced MR imaging. Radiology 2015;274:830-840.

48. Zhang J, Liu H, Tong H, et al. Clinical applications of contrast-enhanced perfusion MRI techniques in gliomas: Recent advances and current challenges. Contrast Media Mol Imaging 2017;2017:7064120-7064127.

49. Leach MO, Morgan B, Tofts PS, et al. Imaging vascular function for early stage clinical trials using dynamic contrast-enhanced magnetic resonance imaging. Eur Radiol 2012;22:1451-1464.

50. Petralia G, Summers PE, Agostini A, et al. Dynamic contrast-enhanced MRI in oncology: How we do it. Radiol Med 2020;125:1288-1300.

51. Harrer JU, Parker GJM, Haroon HA, et al. Comparative study of methods for determining vascular permeability and blood volume in human gliomas. J Magn Reson Imaging 2004;20:748-757.

52. Okuchi S, Rojas-Garcia A, Ulyte A, et al. Diagnostic accuracy of dynamic contrast-enhanced perfusion MRI in stratifying gliomas: A systematic review and meta-analysis. Cancer Med 2019;8:5564-5573.

53. Hu Y, Chen Y, Wang J, Kang JJ, Shen DD, Jia ZZ. Non-invasive estimation of glioma IDH1 mutation and VEGF expression by histogram analysis of dynamic contrast-enhanced MRI. Front Oncol 2020;10:593102.

54. Ulyte A, Katsaros VK, Liouta E, et al. Prognostic value of preoperative dynamic contrast-enhanced MRI perfusion parameters for high-grade glioma patients. Neuroradiology 2016;58:1197-1208.

55. Kim H. Variability in quantitative DCE-MRI: Sources and solutions. J Nat Sci 2018;4:e484.

56. Duan C, Kallehauge JF, Bretthorst GL, Tanderup K, Ackerman JJH, Garbow JR. Are complex DCE-MRI models supported by clinical data? Magn Reson Med 2017;77:1329-1339.

57. Alsop DC, Detre JA, Golay X, et al. Recommended implementation of arterial spin-labeled perfusion MRI for clinical applications: A consensus of the ISMRM perfusion study group and the European consortium for ASL in dementia. Magn Reson Med 2015;73:102-116.

58. Falk Delgado A, De Luca F, van Westen D, Falk Delgado A. Arterial spin labeling MR imaging for differentiation between high- and low-grade glioma-a meta-analysis. Neuro Oncol 2018;20:1450-1461.

59. Soldozy S, Galindo J, Snyder H, et al. Clinical utility of arterial spin labeling imaging in disorders of the nervous system. Neurosurg Focus 2019;47:E5.

60. Abdel Razek AAK, Talaat M, El-Serougy L, Gaballa G, Abdelsalam M. Clinical applications of arterial spin labeling in brain tumors. J Comput Assist Tomogr 2019;43:525-532.

61. Kong L, Chen H, Yang Y, Chen L. A meta-analysis of arterial spin labelling perfusion values for the prediction of glioma grade. Clin Radiol 2017;72:255-261.

62. Alsaedi A, Doniselli F, Jäger HR, et al. The value of arterial spin labelling in adults glioma grading: Systematic review and meta-analysis. Oncotarget 2019;10:1589-1601.

63. Mao J, Deng D, Yang Z, et al. Pretreatment structural and arterial spin labeling MRI is predictive for p53 mutation in high-grade gliomas. Br J Radiol 2020;93:20200661.

64. Yoo R-E, Yun TJ, Hwang I, et al. Arterial spin labeling perfusion-weighted imaging aids in prediction of molecular biomarkers and survival in glioblastomas. Eur Radiol 2020;30:1202-1211.

65. Dangouloff-Ros V, Deroulers C, Foissac F, et al. Arterial spin labeling to predict brain tumor grading in children: Correlations between histopathologic vascular density and perfusion MR imaging. Radiology 2016;281:553-566.

66. Pang H, Dang X, Ren Y, et al. 3D-ASL perfusion correlates with VEGF expression and overall survival in glioma patients: Comparison of quantitative perfusion and pathology on accurate spatial location-matched basis. J Magn Reson Imaging 2019;50:209-220.

67. Flies CM, Snijders TJ, Van Seeters T, et al. Perfusion imaging with arterial spin labeling (ASL)-MRI predicts malignant progression in low-grade (WHO grade II) gliomas. Neuroradiology 2021;63:2023-2033.

68. Yang S, Zhao B, Wang G, et al. Improving the grading accuracy of astrocytic neoplasms noninvasively by combining timing information with cerebral blood flow: A multi-TI arterial spin-labeling MR imaging study. AJNR Am J Neuroradiol 2016;37:2209-2216.

69. Xiao H-F, Chen Z-Y, Lou X, et al. Astrocytic tumour grading: A comparative study of three-dimensional pseudocontinuous arterial spin labelling, dynamic susceptibility contrast-enhanced perfusion-weighted imaging, and diffusion-weighted imaging. Eur Radiol 2015;25:3423-3430.

70. Qu Y, Kong D, Wen H, et al. Perfusion measurement in brain gliomas using velocity-selective arterial spin labeling: Comparison with pseudo-continuous arterial spin labeling and dynamic susceptibility contrast MRI. Eur Radiol 2022;32:2976-2987.

71. Zhang L, Min Z, Tang M, Chen S, Lei X, Zhang X. The utility of diffusion MRI with quantitative ADC measurements for differentiating high-grade from low-grade cerebral gliomas: Evidence from a meta-analysis. J Neurol Sci 2017;373:9-15.

72. Wang C, Xu Z, Wang S, et al. Clinical importance of ADC in the prediction of 125I in the treatment for gliomas. J Cancer 2021;12:1945-1951.

73. Leu K, Ott GA, Lai A, et al. Perfusion and diffusion MRI signatures in histologic and genetic subtypes of WHO grade II-III diffuse gliomas. J Neurooncol 2017;134:177-188.

74. Park YW, Park JE, Ahn SS, et al. Magnetic resonance imaging parameters for noninvasive prediction of epidermal growth factor receptor amplification in isocitrate dehydrogenase-wild-type lower-grade gliomas: A multicenter study. Neurosurgery 2021;89:257-265.

75. Fujita Y, Nagashima H, Tanaka K, et al. The histopathologic and radiologic features of T2-FLAIR mismatch sign in IDH-mutant 1p/19q non-codeleted Astrocytomas. World Neurosurg 2021;149:e253-e260.

76. Thust S, Micallef C, Okuchi S, et al. Imaging characteristics of H3 K27M histone-mutant diffuse midline glioma in teenagers and adults. Quant Imaging Med Surg 2021;11:43-56.

77. Seong M, Kim ST, Noh JH, Kim YK, Kim H-J. Radiologic findings and the molecular expression profile of diffuse midline glioma H3 K27M mutant. Acta Radiol 2021;62:1404-1411.

78. White ML, Zhang Y, Yu F, Jaffar Kazmi SA. Diffusion tensor MR imaging of cerebral gliomas: Evaluating fractional anisotropy characteristics. AJNR Am J Neuroradiol 2011;32:374-381.

79. Luks TL, McKnight TR, Jalbert LE, et al. Relationship of In vivo MR parameters to histopathological and molecular characteristics of newly diagnosed, nonenhancing lower-grade gliomas. Transl Oncol 2018;11:941-949.

80. Xiong J, Tan W-L, Pan J-W, et al. Detecting isocitrate dehydrogenase gene mutations in oligodendroglial tumors using diffusion tensor imaging metrics and their correlations with proliferation and microvascular density. J Magn Reson Imaging 2016;43:45-54.

81. Augelli R, Ciceri E, Ghimenton C, et al. Magnetic resonance diffusion-tensor imaging metrics in high grade gliomas: Correlation with IDH1 gene status in WHO 2016 era. Eur J Radiol 2019;116:174-179.

82. Park YW, Han K, Ahn SS, et al. Whole-tumor histogram and texture analyses of DTI for evaluation of IDH1-mutation and 1p/19q-codeletion status in World Health Organization grade II gliomas. AJNR Am J Neuroradiol 2018;39:693-698.

15222586, 2023, 6, Downloaded from https://onlinelibrary.wiley.com/doi/10.1002/jmri.28662 by Imperial College London, Wiley Online Library on [24/05/2023]. See the Terms and Conditions (https://onlinelibrary.wiley.com/terms-and-conditions) on Wiley Online Library for rules of use; OA articles are governed by the applicable Creative Commons License

83. Bette S, Huber T, Gempt J, et al. Local fractional anisotropy is reduced in areas with tumor recurrence in glioblastoma. Radiology 2017;283:499-507.

84. Raab P, Hattingen E, Franz K, Zanella FE, Lanfermann H. Cerebral gliomas: Diffusional kurtosis imaging analysis of microstructural differences. Radiology 2010;254:876-881.

85. Van Cauter S, De Keyzer F, Sima DM, et al. Integrating diffusion kurtosis imaging, dynamic susceptibility-weighted contrast-enhanced MRI, and short echo time chemical shift imaging for grading gliomas. Neuro Oncol 2014;16:1010-1021.

86. Tietze A, Hansen MB, Østergaard L, et al. Mean diffusional kurtosis in patients with glioma: Initial results with a fast imaging method in a clinical setting. AJNR Am J Neuroradiol 2015;36:1472-1478.

87. Bisdas S, Shen H, Thust S, et al. Texture analysis- and support vector machine-assisted diffusional kurtosis imaging may allow in vivo gliomas grading and IDH-mutation status prediction: A preliminary study. Sci Rep 2018;8:6108.

88. Kikuchi K, Hiwatashi A, Togao O, et al. Intravoxel incoherent motion MR imaging of pediatric intracranial tumors: Correlation with histology and diagnostic utility. AJNR Am J Neuroradiol 2019;40:878-884.

89. Puig J, Sánchez-González J, Blasco G, et al. Intravoxel incoherent motion metrics as potential biomarkers for survival in glioblastoma. PLoS One 2016;11:e0158887.

90. Kiselev VG, Strecker R, Ziyeh S, Speck O, Hennig J. Vessel size imaging in humans. Magn Reson Med 2005;53:553-563.

91. Boxerman JL, Hamberg LM, Rosen BR, Weisskoff RM. MR contrast due to intravascular magnetic susceptibility perturbations. Magn Reson Med 1995;34:555-566.

92. Emblem KE, Mouridsen K, Bjornerud A, et al. Vessel architectural imaging identifies cancer patient responders to anti-angiogenic therapy. Nat Med 2013;19:1178-1183.

93. Kadota T, Nakagawa H, Kuroda C. Malignant glioma. Evaluation with 3D time-of-flight MR angiography. Acta Radiol 1998;39:227-232.

94. Radbruch A, Eidel O, Wiestler B, et al. Quantification of tumor vessels in glioblastoma patients using time-of-flight angiography at 7 Tesla: A feasibility study. PLoS One 2014;9:e110727.

95. Strumia M, Reichardt W, Staszewski O, et al. Glioma vessel abnormality quantification using time-of-flight MR angiography. Magma 2016;29:765-775.

96. Puig J, Blasco G, Daunis-I-Estadella J, et al. High-resolution blood-pool-contrast-enhanced MR angiography in glioblastoma: Tumor-associated neovascularization as a biomarker for patient survival. A preliminary study. Neuroradiology 2016;58:17-26.

97. Kang H-Y, Xiao H-L, Chen J-H, et al. Comparison of the effect of vessel size imaging and cerebral blood volume derived from perfusion MR imaging on glioma grading. AJNR Am J Neuroradiol 2016;37:51-57.

98. Stadlbauer A, Zimmermann M, Kitzwögerer M, et al. MR imaging-derived oxygen metabolism and neovascularization characterization for grading and IDH gene mutation detection of gliomas. Radiology 2017;283:799-809.

99. Zhang K, Yun SD, Triphan SMF, et al. Vessel architecture imaging using multiband gradient-echo/spin-echo EPI. PLoS One 2019;14:e0220939.

100. Stadlbauer A, Zimmermann M, Heinz G, et al. Magnetic resonance imaging biomarkers for clinical routine assessment of microvascular architecture in glioma. J Cereb Blood Flow Metab 2017;37:632-643.

101. Ozsarlak O, Van Goethem JW, Maes M, Parizel PM. MR angiography of the intracranial vessels: Technical aspects and clinical applications. Neuroradiology 2004;46:955-972.

102. Kang C-K, Park C-W, Han J-Y, et al. Imaging and analysis of lenticulostriate arteries using 7.0-Tesla magnetic resonance angiography. Magn Reson Med 2009;61:136-144.

103. Cheng H-LM, Stikov N, Ghugre NR, Wright GA. Practical medical applications of quantitative MR relaxometry. J Magn Reson Imaging 2012;36:805-824.

104. Tanenbaum LN, Tsiouris AJ, Johnson AN, et al. Synthetic MRI for clinical neuroimaging: Results of the magnetic resonance image compilation (MAGiC) prospective, multicenter, multireader trial. AJNR Am J Neuroradiol 2017;38:1103-1110.

105. Ma D, Gulani V, Seiberlich N, et al. Magnetic resonance fingerprinting. Nature 2013;495:187-192.

106. Jiang Y, Ma D, Seiberlich N, Gulani V, Griswold MA. MR fingerprinting using fast imaging with steady state precession (FISP) with spiral readout. Magn Reson Med 2015;74:1621-1631.

107. Badve C, Yu A, Dastmalchian S, et al. MR fingerprinting of adult brain tumors: Initial experience. AJNR Am J Neuroradiol 2017;38:492-499.

108. de Blank P, Badve C, Gold DR, et al. Magnetic resonance fingerprinting to characterize childhood and young adult brain tumors. Pediatr Neurosurg 2019;54:310-318.

109. Kern M, Auer TA, Picht T, Misch M, Wiener E. T2 mapping of molecular subtypes of WHO grade II/III gliomas. BMC Neurol 2020;20:8.

110. Mariappan Y, McGee K, Ehman R. Quantitative MRI of tumors. *Quantifying morphology and physiology of the human body using MRI*. Boca Raton, FL: CRC Press; 2013. p 283-342.

111. Dastmalchian S, Kilinc O, Onyewadume L, et al. Radiomic analysis of magnetic resonance fingerprinting in adult brain tumors. Eur J Nucl Med Mol Imaging 2021;48:683-693.

112. Springer E, Cardoso PL, Strasser B, et al. MR fingerprinting—A radiogenomic marker for diffuse gliomas. Cancer 2022;14:723.

113. Blystad I, Warntjes JBM, Smedby Ö, Lundberg P, Larsson E-M, Tisell A. Quantitative MRI for analysis of peritumoral edema in malignant gliomas. PLoS One 2017;12:e0177135.

114. Blystad I, Warntjes JBM, Smedby Ö, Lundberg P, Larsson E-M, Tisell A. Quantitative MRI using relaxometry in malignant gliomas detects contrast enhancement in peritumoral oedema. Sci Rep 2020;10:17986.

115. Nöth U, Tichy J, Tritt S, Bähr O, Deichmann R, Hattingen E. Quantitative T1 mapping indicates tumor infiltration beyond the enhancing part of glioblastomas. NMR Biomed 2020;33:e4242.

116. Pirkl CM, Nunez-Gonzalez L, Kofler F, et al. Accelerated 3D whole-brain T1, T2, and proton density mapping: Feasibility for clinical glioma MR imaging. Neuroradiology 2021;63:1831-1851.

117. Körzdörfer G, Kirsch R, Liu K, et al. Reproducibility and repeatability of MR fingerprinting relaxometry in the human brain. Radiology 2019;292:429-437.

118. McGivney DF, Boyacıoğlu R, Jiang Y, et al. Magnetic resonance fingerprinting review part 2: Technique and directions. J Magn Reson Imaging 2020;51:993-1007.

119. Menze BH, Jakab A, Bauer S, et al. The multimodal brain tumor image segmentation benchmark (BRATS). IEEE Trans Med Imaging 2015;34:1993-2024.

120. Bell L, Mutsaerts H-J, Fedorov A, et al. Open source initiative for perfusion imaging (OSIPI): A profile on a community led initiative. *2021 ISMRM & SMRT Annual Meeting & Exhibition*. Concord, CA: International Society for Magnetic Resonance in Medicine; 2021.

121. Shukla-Dave A, Obuchowski NA, Chenevert TL, et al. Quantitative imaging biomarkers alliance (QIBA) recommendations for improved precision of DWI and DCE-MRI derived biomarkers in multicenter oncology trials. J Magn Reson Imaging 2019;49:e101-e121.

122. Mahroo A, Buck MA, Huber J, et al. Robust multi-TE ASL-based blood-brain barrier integrity measurements. Front Neurosci 2021;15:719676.

15222586, 2023, 6, Downloaded from https://onlinelibrary.wiley.com/doi/10.1002/jmri.28662 by Imperial College London, Wiley Online Library on [24/05/2023]. See the Terms and Conditions (https://onlinelibrary.wiley.com/terms-and-conditions) on Wiley Online Library for rules of use; OA articles are governed by the applicable Creative Commons License